MASTER'S THESIS

Alternative Process for Ceramic Based Composite Materials Elaboration

Caroline Liegaut
2014

Master of Science in Engineering Technology
Materials Technology (EEIGM)

Luleå University of Technology
Department of Engineering Sciences and Mathematics

LULEÅ UNIVERSITY OF TECHNOLOGY

ACKNOWLEDGEMENTS

First, I would like to express my sincere gratitude to Francis TEYSSANDIER for letting me integrate his laboratory where I could realise my internship in the best conditions.

I am particularly thankful to Brice TAILLET, for giving me the opportunity to realise my master thesis internship at the LCTS (Laboratoire des Composites Thermo-Structuraux); for his help all along the project, his advices, his good mood, thanks to him I have learnt a lot on scientific and human points of view. And even if you stay the greatest card-sharp during “belote” games, it was a real pleasure to work with you. I could not have found a better supervisor!

Also, thanks to René PAILLER, research engineer for CNRS (Centre National de la Recherche Scientifique) and Brice’s PhD supervisor, and Bernard REIGNIER, HERAKLES engineer, for the administrative procedures, in order for me to start my project at the fixed date.

Thanks to the PhD students, all personnel, researchers and technicians. Thanks to all the people that have eaten with me every lunch, for the laughs and great moments we had.

I would like to thank all the other interns who worked at the same time as me at the laboratory, especially Clio, Pierre, Lorie, Simon, Anne, Titouan, Cindy, Jocelin and Matthieu L., for the good times spent together in and out of the laboratory.

Finally, thanks to Professor Marta-Lena ANTTI, for accepting to be my supervisor at LTU, Sweden. Thanks to Viola NILSSON, for her help in administrative procedures. And also, Zoubir AYADI, responsible of the industrial relations at the EEIGM (Ecole Européenne d’Ingénieurs en Génie des Matériaux) in Nancy, first for sharing the internship offer and also for the help he provided me to be able to validate my French-Swedish double diploma.

Tack för allt, och vi ses!

Pessac, France, July 2014

Caroline Liégaut

ABSTRACT

Nowadays, the civil aeronautic industry is subjected to many standards aiming to the reduction of its environmental impact. This leads industries to elaborate new materials, lighter and more efficient, to replace for example parts of the turbojets which are currently made of nickel based super-alloys. Thermostructural composites, and more specifically ceramic matrix composites (CMC), are promising materials in this domain due to their low density, mechanical properties and their resistance to oxidation in a wide range of temperatures. The present work has been focused on the optimisation of a new matrix material by an innovating elaboration process, to be able to reach temperature in use greater than 1450°C.

3D woven preforms made with Hi-Nicalon S fibres were used. Depending on the porosity size distribution, filling by submicron powders suction required a powder suspension with a controlled particle size range. Wet ball milling led to particle size between 0.6 and 0.8 µm, which allowed the filling of 50 to 55% of the initial porosities with a 18 vol% charged suspension.

Then, the preforms were densified by a pressurised heat treatment. Heating rate and pressure were controlled by self-regulation programs. The synthesis reaction has also been controlled and monitored by an acquisition program of the temperature at the surface of the material.

The different characterization techniques that have been used, allowed a better understanding of the physical and chemical properties of the prepared samples, and thus a study of the influences of the manufacturing parameters. Scanning electron microscopy (SEM) observations showed that the fibres were not damaged despite the high temperature during treatments. Moreover, a good cohesion between matrix and consolidation has been observed. They also revealed that for low heating rate, non-reaction zones in the matrix could be seen. At constant pressure, different heating rates were tested. The X-ray diffraction (XRD) analysis showed an increase in the mass content of the desired compound while heating rate was increasing.

Thermograms recorded during treatments showed three phenomena linked to the pressure variation:

- Greater the pressure, lower the initiation temperature of the reaction
- The range of the exothermal peak is proportional to the gas pressure
- Greater the pressure, the more intense and quicker the reaction

Finally, an optimal combination of pressure and heating rate leading to the synthesis of the desired matrix compound could have been determined to achieve a 95% in mass in function of the preform type. Mechanical characterisation and wet oxidation aging are still to be carried out to have a better understanding of the behaviour of the composite materials that have been made.

TABLE OF CONTENTS

INTRODUCTION

Since many years, composite materials allowed the development of aeronautic, military and spatial industries, and their applications are still expanding, as well as their quality and performance level. They have been adapted to the level of requirements imposed by the civil aeronautics. Indeed, one of the principal benefits of these materials is their lightness compared to those of metals, which have been mainly used in aircraft's production since the beginning of the aviation era.

Today, sustainable development is part of the main preoccupations of governments and industries. That is why they have launched different research programs and put in place new standards and measures with national, European and international scope, aimed at reducing the environmental impacts caused by the production and use of airplanes across the world.

Present needs, linked to programs like Clean Sky (http://www.cleansky.eu/), FlightPath 2050 or ACARE (http://www.acare4europe.org/), are linked to the energy consumption reduction, or environmental impacts such as noise and pollution. Researches are focused on reducing the weight of the structures by using composite materials, but depending on the application and the technologies involved, their production cost and the materials used can reach high prices. So that it is important to be able to develop those new materials with competitive and attractive methods.

Trusting the evolution of the use of composite materials in aeronautics, it can be observed that the proportion is still more important, reaching today with the Airbus A350 a bit more than 50% of the structure weight. Organic matrix composites are the most used for the fuselage (aircraft main body), wings and empennages (tail assembly). The air traffic projections announce its doubling over the next twenty years. The introduction of new composite materials in other parts of airplane is necessary to propose a mean of transportation respecting these new norms and demands. For example, aircraft engines are still produced with alloys. Industrial innovations and progresses have been used to develop new processes and tools that are being improved to develop composites with better properties for parts with complex geometry like turbine blades and parts in the combustion chambers.

The materials, which have excellent mechanical, physical and chemical properties, are the thermostructural composites (TSC). Their use in jet engine could favour the access to the civil aviation market with increased performances and reaching of the objectives given by the different European standards and measures in terms of polluting emissions. Composed by carbon or ceramic fibres combined with carbon or ceramic matrix, they have the advantage to keep their mechanical properties at very high temperature, which underlines the interest of their use in turbojet.

One of the main aims of this internship, and the thesis in which it takes part, is to reduce the production costs by optimising an innovative and new prodution method which involves different processes. This could at the same time reduce different impacts of the production and also allow to have a sufficient rate of production to stay competitive as it is needed for the civil aeronautic industry [Taillet, 14]. The use of new materials and new elaboration techniques for these CMCs set certain limits to the experimental approach. It is important to determine quickly which elaboration

parameters are influencing the properties and in which way, to be able to limit the experiences and to use the limited time efficiently to give conclusive results.

In the first part, the state-of-the-art is done on the technological advances and the ceramic matrix composites, to have the maximum of information on the processes already used, and their pros and cons. Then the materials and elaboration techniques will be presented in order to explain the choices and to detail the procedures that have been followed during this work. The part that follows will focus on the characterisation of these new materials, which was an important part of the work that have been realised, the different analysis will be explained. The results will be discussed and compared to each other, to demonstrate the influence of the different elaboration parameters but also to prove the repeatability of the results and validate the methods that have been used. Finally a conclusion will be given on the different tested approaches and some ideas for possible future researches will be proposed.

Because of the confidentiality of the subject and the patent deposition linked to this work, no compounds names or elaboration methods which are explained in the patent will appear in this report. Also, scales on pictures will not appear, that's why no appendices are added because they are not giving more information or details.

I- LITERATURE REVIEW

I.1) Overview on composites materials

A material can be qualified as a composite when it is made from different constituents that are combined to obtain better properties and characteristics than individual constituent.

Three different composites families exist: organic matrix composites (OMC), metal matrix composites (MMC) and ceramic matrix composites (CMC). The choice of the constituents highly depends on the temperature in use. For each type of composite, there are the reinforcement (for example fibres or particles) which ensures the mechanical performances; eventually an interphase, and the matrix. In the case of CMC, the matrix ensures the global cohesion of the structure and allows the good transmission of mechanical stresses subjected to the materials.

Technical and scientific advances helped the improvement of the composite elaboration processes and their properties, and so allow their use in more and more industrial domains.

I.2) Ceramic matrix composites (CMC)

I.2.1) Background on ceramics

Ceramics appeared during the Neolithic age and was part of the first man made materials developed from clay and thanks to the control of fire. They were mainly used for domestic products and building materials. Then engineering ceramics were developed thanks to the evolution of knowledge and know-how, and also the special needs of certain industries. They can be found today in medical, electronic, aeronautic and spatial applications.

These materials are non-metallic and inorganic, they need high manufacturing temperatures. The engineering ceramics are now made from oxide, carbide or nitride materials. These new ceramics are almost fully crystallised, even if there are still some amorphous zones. Their atomic structures are complicated. Indeed, almost all the electrons are contributing to strong chemical bonding, which is a combination of ionic and covalent bonds which proportions depend on the difference of electronegativity between atoms. This is the reason why their physical and chemical properties are good, such as excellent thermal and chemical stability, but also high theoretical mechanical resistance and hardness [Lécrivain, 87].

Their mechanical properties are varying depending on the temperature. Their behaviour at low temperature is brittle due to their low strain at break, low toughness and impact (shock) resistance. Their properties remain constant up to 1400-1500°C, as it is the case for silicon carbide (SiC) [Baïlon, 00], unlike metals that have decreasing properties with the increase of temperature. Ceramics show a better mechanical and thermal shock resistance due to their good properties. Moreover, they are good insulator because they have usually a low thermal conductivity.

These good properties make these ceramics very attractive as structural materials and more specifically in the aeronautic and spatial domains in which the materials have to resist to severe thermal and mechanical stresses in oxidant environment. Despite their brittleness, researches focused on increasing their performance of cracking resistance. Several solutions were found like defects reduction in ceramic materials to increase mechanical resistance. But there are so many production steps that can introduce these defects, that researchers determined ceramic based composites as a solution allowing the presence of few defects in the ceramic microstructure.

I.2.2) The different constituents of CMC

The CMCs are composed by refractory fibres and a ceramic matrix. These materials show interesting characteristics such as lightness, good mechanical resistance and chemical stability at high temperature. Like all other types of composites, they are composed by different elements that bring different properties to the material:

- Reinforcements :

Particles are generally used to improve special properties like thermal or electrical conductivity. Long or short fibres are improving the mechanical behaviour of the material. Short fibres improve toughness and reduce the dispersion of the stress at break [Wang, 98]. Long fibres ensure good stiffness and breaking resistance because they are supporting the most of the mechanical stresses.

These fibres are different in their length, but they can also be different depending on their placement (1D assembly, 2D or 3D woven, or 3D needle punching nonwoven fabric) and also depending on their nature [Dupeux, 04], [Gay, 97], [Christin, 05]. Long fibres are described in particular. Carbon fibres or silicon carbide fibres (SiC) are the most used in CMC production, and have been chosen for their lightness, stiffness, thermal and chemical stability, and their ease of weaving. Carbon fibres are cheap and have excellent thermal stability and conductivity, but are sensitive to oxidation from 400°C. Silicon carbide fibres are more tough and oxidation resistant [Naslain, 03]. There are other types of fibres like oxide fibres which can be inert in oxidant atmosphere. But when temperature is higher than 1000°C, their properties are decreasing and are no longer interesting [Bunsell, 00].

Table 1 groups together some advantages and disadvantages of different types of ceramic fibres [Eberling-Fux, 06] [Naslain, 03] [Naslain, 05] [Bunsell, 05].

Nature	Advantages	Disadvantages
Oxide	- Inert in oxidant atmosphere	- Drop of mechanical properties at high temperature - Grain growth and creep from 1000°C - Thermal insulation - Higher density than for C and SiC fibres
Carbon	- Excellent thermo-mechanical properties - Good thermal conductivity - High modulus fibres or high strength fibres - Low density: 1.7 to 2 - Ease of weaving - Low cost	- Oxidation sensitivity from 400°C
Silicon carbide	- Excellent mechanical properties at high temperature - Low density : 2,5 à 3,2 - Passive oxidation from 800 to 1500°C if partial pressure of oxygen is greater than 100Pa	- Weaving difficulties because of good stiffness - Thermal stability lower than for carbon fibres - Optimal elaboration temperature needed because of the fibre type - Expensive

Table 1 : Advantages and disadvantages of ceramic fibres mainly used in CMC materials.

The first SiC fibres have been created in the 1970's by Yajima et al. [Yajima, 76], [Yajima, 78], and were commercialised under the name Nicalon by the Japanese company Nippon Carbon. They are made by crosslinking and pyrolysis of organosilicon precursor filaments, and more precisely polycarbosilane (PCS). This process is divided into three main steps: spinning of melted PCS at 300°C in an inert atmosphere to obtain organometallic fibres, then crosslinking by oxidation in order to make the fibres infusible and finally pyrolysis at 1200°C in inert atmosphere leading to the desired ceramic fibres. Nicalon fibres are thermodynamically unstable above 1100°C because of the presence of a Si-O-C phase that is decomposing [Bouillon, 91].

The improvement of the thermal stability of first generation fibres is linked to the improvement of the manufacturing processes that are introducing oxygen and are leading to a high free carbon rate. The Hi-Nicalon fibre was developed with a similar process as for Nicalon fibres; only the oxidation crosslinking step was replaced by an electron irradiation crosslinking in inert atmosphere. There was no longer amorphous Si-O-C phase and the fibres were remaining stable up to 1400°C [Takeda, 95]. Nevertheless, there is still an excess of free carbon that makes the Hi-Nicalon fibre sensitive to oxygen and creep [Chollon, 95].

Third generation fibres were finally made aiming to pure SiC fibres that resist to creep. Free carbon rate is much lower because pyrolysis conditions were modified. Unlike Hi-Nicalon that are pyrolysed in void at 1300°C, Hi-Nicalon S fibres are pyrolysed in hydrogen atmosphere at 1600° [Ichikawa, 00].

Table 2 groups together some SiC based fibres characteristics [Papakonstantinou, 01] [Naslain, 04] [Bunsell, 06].

Fibre type	Nicalon	Hi-Nicalon	Hi-Nicalon S
Diameter in µm	15	14	12
% O	12	0.5	0.2
C/Si ratio in %at	1.32	1.41	1.05
SiC grain diameter in nm	2	5	12
Young's modulus in GPa	200	270	420
Ultimate tensile strength in MPa	3000	2800	2600
Price in $/kg	200	8000	13000

Table 2 : Nicalon fibres characteristics

Fibrous structures can have different textures, fibres architectures. 2D structures are obtained by weaving or making laminates by pilling up different unidirectional layers with different orientation [Christin, 02]. However, their poor interlaminar strength causes delamination during fabrication or testing, but it can be improved by intertwinning rods to make preforms or by interlocking to consolidate the different layers together. This needling technology consists of attaching successive cloth and fibre layers together with fibres carried by hooks-fitted needles crossing the layers [Christin, 05]. These new structures can be 3D or nD and present a better isotropic behaviour. Studies showed that it had improved their permeability for a better densification, but also their resistance to interlaminar shear.

- The interphase :

This interphase is found between the matrix and the fibrous reinforcement. Its thickness is usually between 100 and 500 nm, it helps the interaction between fibres and matrix so that the final composite is not brittle, knowing that its constituents are intrinsically brittle. It can also make the crack deviate in parallel to the stress direction, protecting the fibres from a premature failure (figure 1, [Taillet, 14]), ensuring the mechanical efforts transfer between fibre and matrix, it can also limit residual stresses due to manufacturing processes and it can help to keep good properties at high temperatures.

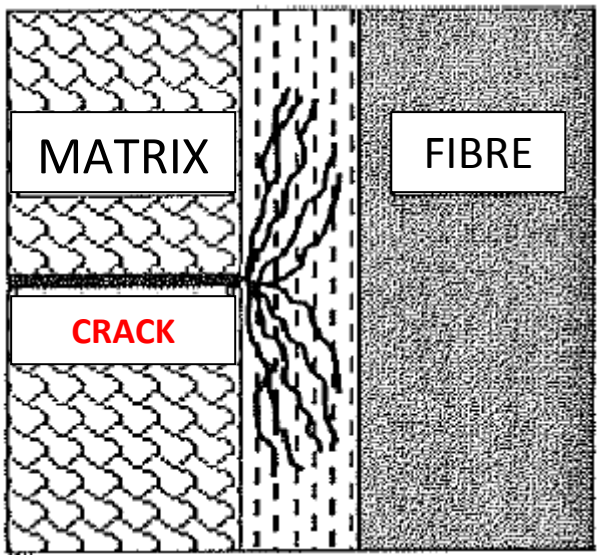

Figure 1 : Principle of deviation of cracks by the interphase

Depending on the fibre-matrix bonding quality, several mechanical behaviours can be observed as shown on figure 2 [Cabrero, 09] [Naslain, 04] [Naslain, 05]:

- Weak bond : fibre-matrix decohesion, same behaviour as fibres on their own
- Strong bond : brittle behaviour, crack propagation to fibres
- Intermediate bond : pseudo-ductile behaviour, progressive multicracking of the matrix and then efforts transfer from matrix to fibres, greater ultimate tensile strength

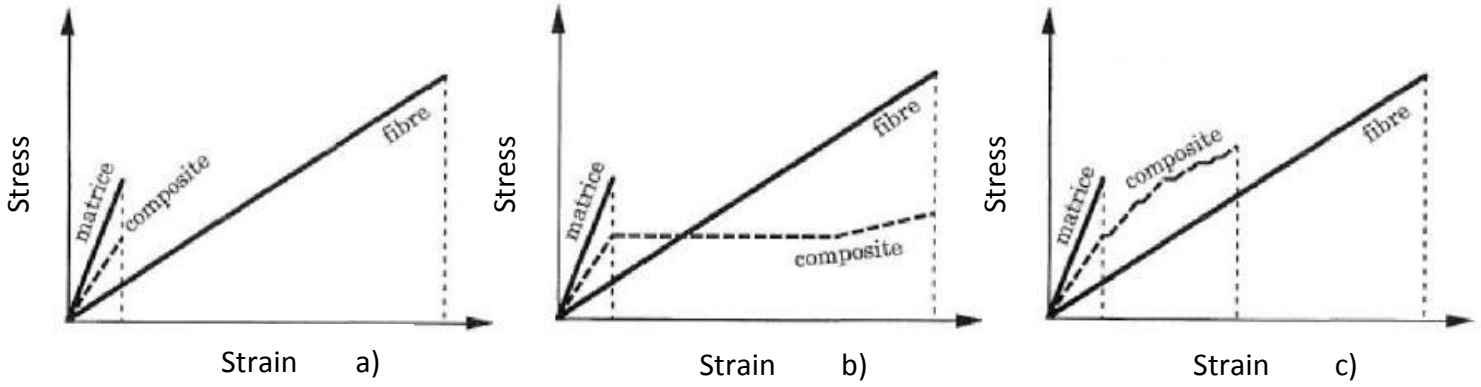

Figure 2 : Traction behaviour of a CMC depending on the fibre-matrix interface quality; a) strong bond, b) intermediate bond and c) weak bond.

The interphase should have a good physical and chemical compatibility with the fibres and the matrix, be highly anisotropic and have a low shear resistance. Pyrocarbon and boron nitride have a lamellar microstructure and are ideal materials for CMC.

PyC (pyrocarbon or pyrolytic carbon) is the most used. It is formed on the fibres by chemical vapour infiltration (CVI) by pyrolytic cracking of gaseous hydrocarbons. Its resistance to oxidation lowers above 400°C; hence a matrix that acts as an efficient oxidation protection is needed.

Boron nitride has a better oxidation resistance than PyC, it starts oxidizing from 600°C. At this temperature, it forms liquid boron oxide B_2O_3 that dissolves SiC and leads to the formation of a borosilicate glass which allows closing over the microcracks while it is hot and avoids the access to fibres by oxygen for a better protection.

- The matrix :

It ensures the global cohesion of the whole material. It protects, chemically and mechanically, the fibres and the interphase from the outside environment, and mainly ensures the load transfer while holding the reinforcement along the favoured loading axes. The matrix choice depends on the thermal compatibility between the matrix and the reinforcement. High temperatures reached during manufacturing and too distant thermal expansion coefficients values could cause residual stresses. Cracks could open and turn into propagation ways for oxidant species [Naslain, 98].

CMC composition and constituents varied with technical and scientific advances. Carbon fibres reinforced with carbon matrix (C_f/C_m) were the first thermostructural composite material to be used because of its lightness and good mechanical properties. But it is too sensitive to oxidation which is limiting its long use at high temperature.

Then composite materials like C_f/SiC_m and SiC_f/SiC_m were developed to solve this problem combining them sometimes to carbides and nitrides. So that oxidation starts at higher temperature, with a first passive phase during which silica layer is formed, slowing down oxygen transfer inside the materials. Presence of other carbides like TiC or ZrC can make this silica layer porous and alter its protective character [Tampieri, 92] [Shimada, 95].

Even if SiC matrix remains the most used, multilayers matrices called self-healing matrices can improve the oxidation protection and increase the duration of use in oxidant atmosphere [Lamouroux, 99]. This type of matrix is formed layer by layer by gas processes (see figure 3). Elements such as boron or silicon are introduced to lead to the formation of glasses during oxidation (SiO2 or B2O3) more or less fusible depending on their composition. These glasses are filling the microcracks of the matrix under loading by capillarity, slowing down the oxygen infiltration [Naslain, 99].

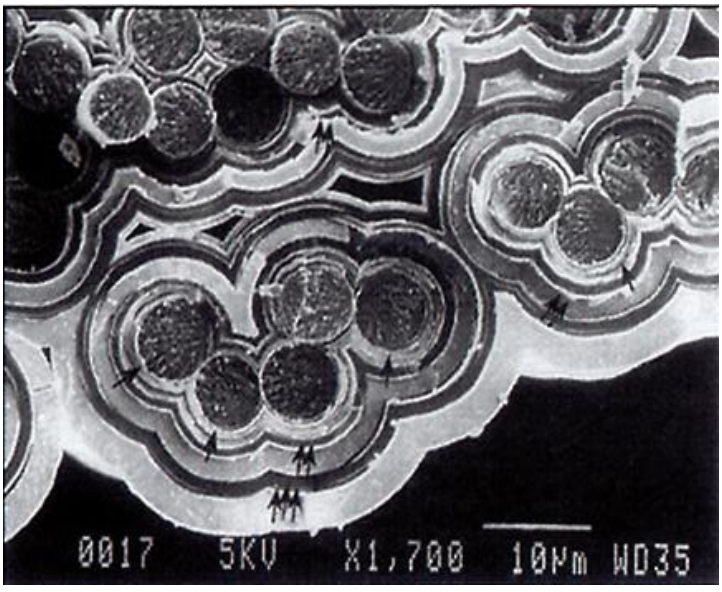

Figure 3 : Transverse section of a multilayered matrix composite

I.2.3) Manufacturing of ceramic matrix composite materials

Depending on the fibrous reinforcement, different manufacturing processes can be used to densify the CMC without altering the reinforcement. Gas, liquid and ceramic processes are mainly used.

- Gas processes :

Chemical vapour infiltration, or CVI, is the process used for this type of materials. The constituents, like the interphase or the matrix, are deposited successively from the decomposition of gaseous precursors at moderate temperature around 900 and 1100°C and at low pressure. Layers are deposited on the fibre surface through the porous structure. The hot fibre surface is used like a substrate where gas or gas mixture is reacting to form a solid which is a thermodynamically stable phase [Choy, 03] [Naslain, 04]. For example, silicon carbide is formed from methyltrichlorosilane (MTS) using hydrogen as carrier and reducing gas. Alkanes are used to form carbon, and carbide or nitride matrices are obtained from more complicated gas mixtures.

It is a slow process, because the deposition rate has to be low enough in function of the gas diffusion rate to form the densest material. It is also necessary that the gas have a continued access to the porosity to be able to react at the heart of the material and not only on the surface. Other CVI-processes were developed:

- Forced flow CVI : the reactive gas are forced to flow through the preforms ;
- Thermal gradient CVI : gas pathways on the surface are longer opened to allow a better deposition in the core of the preforms ;
- Pulsed CVI: repeated steps of evacuation of the deposition chamber, injection of reactant gas and a holding period for deposition to occur; possibility to realise multi-layered matrices [Naslain, 01].

I-CVI, isothermal-isobaric CVI, is the most used process because it can allow deposition on different variety of preforms and on many preforms at the same time. At low temperature under low flow and pressure, gaseous precursors are passing through the preforms by diffusion and this avoids closing the pores [Naslain, 04].

Resultant CMC materials have excellent mechanical properties but they have nevertheless a significant residual porosity rate of 10 to 15%, which can have bad consequences if oxidation occurs and if the matrix is not a self-healing one. The slowness of the process imposes long duration of manufacturing which can reach several weeks of treatment. All the different steps of machining and all the investments needed to reach an efficient production rate are ending up on the high prices of these materials.

- Liquid processes :

  There are two main processes:

  - The impregnation by a metal without reacting (MI, melt infiltration) or reacting (RMI, reactive melt infiltration): This process is used when one of the constituents of the ceramic matrix has low fusion temperature and when it can wet the fibres, like aluminium (Tf=650°C) [Kevorkijian, 99] or silicon (Tf=1416°C) [Luthra, 93]. Only thermally and chemically stable fibres can be impregnated. This impregnation is done by capillarity in the fibrous structure. The reaction leading to the matrix formation is induced by reactive elements deposited on the fibres surface, by impregnation and pyrolysis of an organic resin or with a suspension. In silicon case, RMI leads to a dense composite, but refractoriness and mechanical properties are altered because of the significant amount of residual silicon, hence a limited use to a maximum temperature of 1300°C.

  - Impregnation and pyrolysis of organometallic precursor (PIP, polymer infiltration and pyrolysis): Pyrolysis of organosilicon precursors, already used to produce fibres, has been adapted to ceramic matrix composite manufacturing at the end of the 1990's. The impregnation of the preforms by the preceramic resin is done under vacuum or by RTM (Resin Transfer Moulding) and then appropriate heat treatments are applied to turn the resin into ceramic [Ziegler, 99]. An *in situ* crosslinking of the precursor is usually realised between 200 and 250°C, with or without catalyst. The network obtained by crosslinking is then treated by conventional or micro-waves heating systems [Dong, 02]. The nature and crystallinity of the matrix depend on the pyrolysis temperature, heating rate and atmosphere [Gumula, 04] [Duan, 12]. Polycarbosilane resins (PCS) produce Si-O-C phase matrices whether polysilazane resins (PSZ) are forming Si-C-N phases and under certain conditions can produce a Si_3N_4 matrix [Greil, 00] [Qi, 05]. Several successive PIP cycle are needed to achieve low residual porosity rates because of the important shrinkage due to the heat treatments.

- Ceramic processes :

Usually these processes need the introduction of powders inside the porous preforms, heat treatments to consolidate the structure like sintering, hot isostatic pressing or uniaxial compression. The powders are directly determining the matrix nature. Sintering is generally made at high temperatures combined with pressure; this can damage the reinforcement. The easiest way to introduce the powders in the whole preform is the impregnation under vacuum in a stabilized suspension with a viscosity low enough to allow a good filling of the pores. Submicron powder suction is the most efficient method, because it forces the suspension to go through the preform by applying pressure and/or vacuum. The powders are retained by a filter placed under the preform. After drying of filled preforms, a densification step is needed.

Combination of different gas, liquid and ceramic processes, allows the optimization of the densification. These hybrid processes can be faster and cost saving. Extensive investigations have to be done to improve the industrial methods linked to their combination.

The matrix can be made by all these different techniques. In all cases, the choice of the materials is really important, because they have to be chemically compatible, but also their thermal expansion coefficients have to be close. Their mechanical properties and corrosion resistance have to remain steady with temperature increase. Finally, choice of processes is done depending on the desired materials.

I.2.4) Mechanical properties of CMC

Different parameters can influence the mechanical behaviour of CMC, like the constituents' nature, the interface quality between fibre and matrix, the temperature in use, the atmosphere and the residual porosity.

Depending on the fibre type, wet air oxidation treatments at different temperatures showed the evolution of the ultimate tensile strength in function of temperature [Takeda, 98]. Nicalon fibres have a steady ultimate tensile strength up to 800°C even with their oxygen content limiting their use at high temperature. Hi-Nicalon fibres with less oxygen are stable up to 1300°C. The purity of the Hi-Nicalon S fibres is seen in the mechanical testing which shows a good resistance while temperature is increasing. Usual CMC have an opposite behaviour compared to organic matrix composite (OMC) materials.

The scheme in figure 4 presents the usual three areas observed on mechanical curves of stress in function of strain. Area a) shows a linear part corresponding to the deformation of the matrix and fibres of the composite. Part b) is non-linear and is corresponding to the matrix cracking from a certain stress level. Then when the matrix cracking has been completed, another linear part c) appears when the fibres are taking over the mechanical loading. At point d) the composite failure is observed.

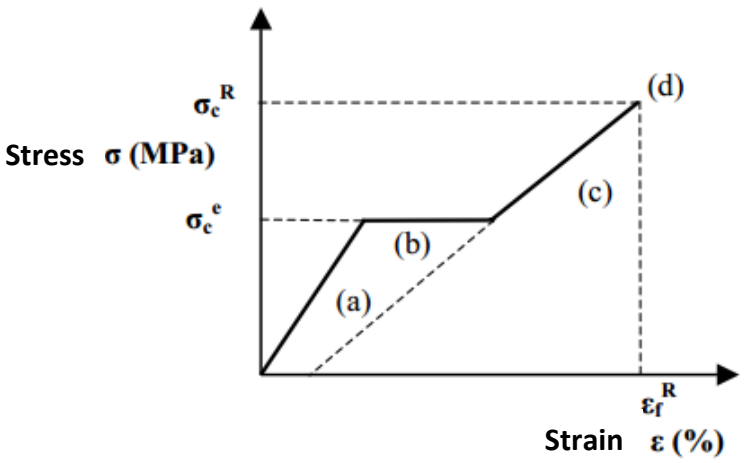

Figure 4 : Theoretical behaviour in traction of a 1D composite

Stress-Strain curves are showed on figure 5; they are showing loading-unloading cycles at room temperature. One can notice the damaging of the composite and the presence of low residual deformation at zero stress. Decrease of Young's modulus and the evolution of hysteresis loops correspond to an interface decohesion, cracking or weakest fibres breaking [Penas, 02].

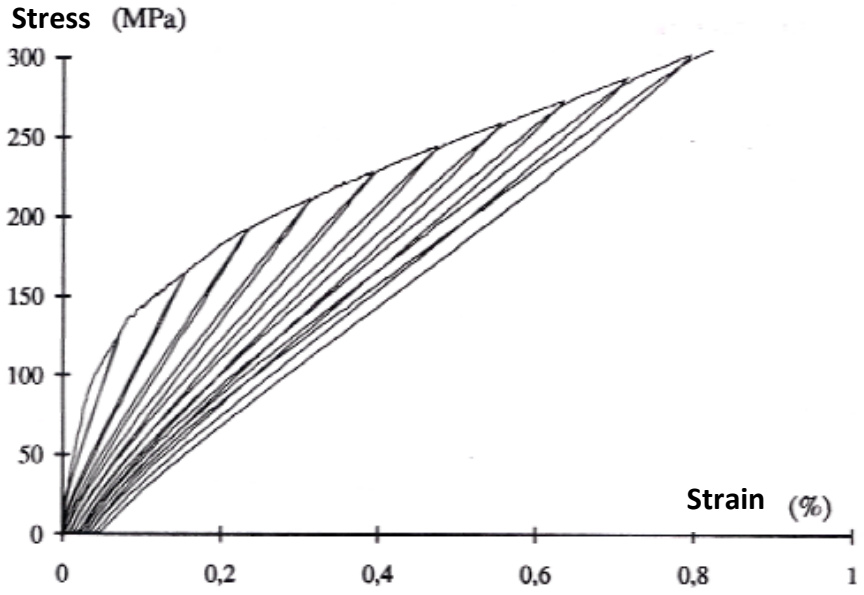

Figure 5 : Loading-unloading cycles on a SiC/SiC composite at room temperature

I.3) Applications of Thermostructural composites (TSC)

CMC reinforced by long or continuous fibres have a promising future, because in this case, fibres mainly improve the mechanical behaviour of the materials. There are some lightweight and high strength fiber reinforced composites that can withstand very high temperature, they are called thermostructural composites (TSC). In this group of composite materials can be found CMC's and also C/C composites. They have a better tolerance to thermal and mechanical damaging at high temperature.

Non-oxide composites can be used as structural parts reaching high temperatures up to 1500°C. They are mainly used in aerospace, aeronautical and military industries, but also in energy and now, civil aviation industries. The new airplanes are subjected to more and more rigorous norms especially on the reduction of pollutant emissions and noise levels. Materials see their mass decreasing and the jet engines efficiency has to be improved.

Currently hot parts of engines are made of nickel based superalloys with a mean density of 8 to 9g/cm^3. They are efficient but complicated to produce and limited to a temperature of 1100°C during their use. CMC have the advantages to be lighter and more refractory, their use could help reducing the mass and have a better control on the combustion to limit pollutant species production.

SiC/SiC composites made by CVI are the most developed and some companies like Herakles showed their good performances on a lot of parts:

- Combustion chambers and exit cones of propellant rocket motors
- Thermal protection for spacecraft
- Flaps, nozzles for airplanes' jets

An ejection cone made of CMC produced by Safran has been tested in 2012 during the first flight test of the Airbus A320 MSN001, and that was also the first use of this part on a civil aircraft. The start-up of use is expected in 2019. One of the main technological challenges for airplanes' jets manufacturers is the production of turbine blades made of CMC. Their low dimensions and complicated geometries are requiring high precision for these parts. Use of SiC/SiC by CVI is also planned on nuclear reactors due to the good resistance to radiations of the SiC β-phase, their excellent failure resistance at high temperature, resistance to creep, corrosion and thermal shocks.

I.4) Conclusions

This literature review exposed the advances in ceramic matrix composite materials domain. A composite material is defined as a material that can benefit of the good properties of its constituents. A monolithic ceramic is brittle and allows no damaging, whereas it can tolerate damaging when it is combined to other elements like in a composite.

Thermostructural composite materials have a low density, interesting mechanical properties and oxidation resistance on a wide range of temperature. These are the reasons why TSC can be used to replace the nickel based superalloys which are limited to 1100°C in use and need cooling systems.

The introduction in the competitive civil aeronautics market induces cost and time constraints, because current production of CMC by CVI is not compatible with high production rates which are necessary to stay competitive in this activity area. Moreover, duration of use in civil airplanes are much greater, materials must be adapted to reach lifetime between 30 000 and 100 000 hours, and not only few minutes as it is needed in space or military applications.

Different alternative processes to replace CVI are presently studied, but the materials that have already been produced are presenting several significant flaws limiting their use to 1300°C. This internship, which is presented in this report, is taking part in a doctoral thesis on the following topic "elaboration of new matrix for thermostable CMC up to 1450°C associated to new processes combination".

A literature review has also been done on the new matrix constituents properties and processes linked to their elaboration, and that have been used to realize some of the samples. But the industrial secrecy imposes not to communicate on these elements.

II- MATERIALS AND METHODS

II.1) Materials

II.1.1) Fibres reinforcement

Ceramic matrix composites had a faster development thanks to the production of silicon carbide fibres. Since the 1970's, different SiC fibres generations had followed one another, of which the last generation with has quasi-stoichiometric compositions, for example the Hi-Nicalon S fibres produced by Nippon Carbon. Even if the oxidation stays one of their limits, they have an excellent resistance at high temperature and to creep. These fibres are composed of SiC, C and O. They can have a diameter between 12 and 13 µm and a density of 3.0 g/cm^3. Their mechanical properties are changing in function of temperature; at room temperature their Young's modulus is around 375 GPa, a strain at break of 0.65% and an ultimate strength of 2.5 GPa. Up to 1000°C, they can start to change and then up to 1400°C properties are dramatically decreasing [Bunsell, 00], [Bunsell, 05]. They are made from polycarbosilane (PCS) treated by electron irradiation or gamma rays, and then pyrolysed under helium atmosphere above 1500°C, the aim of this last process is to reduce the oxygen content [Takeda, 99].

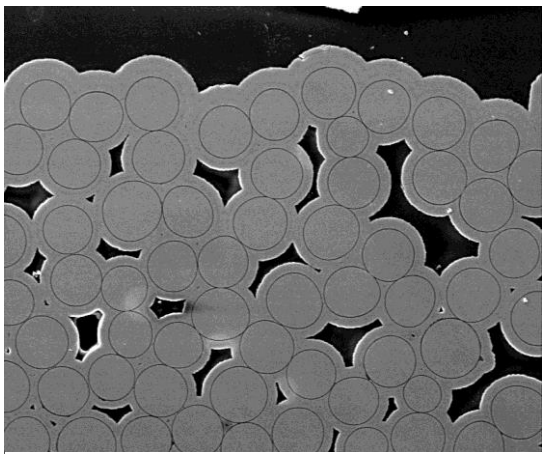

Figure 6 : SEM picture of the fibres consolidated with a SiC layer deposited by CVI in a non-impregnated preform.

In this work, Hi-Nicalon S fibres have been used to make 3D woven preforms. As it is shown on the SEM picture on figure 6, fibres are covered by a pyrocarbon (PyC) interphase and a SiC consolidation and protective layer. Two types of preforms were studied, only the SiC layer thickness is varying, they will be called type 1 and type 2 (with greater thickness than for type 1) in the following parts.

II.1.2) Reactive powders

Two powders, A and B, have been used experimentally. They are commercialised by Sigma-ALDRICH Company and are pure up to 99%. Powder A, as received, has a particle-size distribution from 0.5 to 10 µm, of which 80% is between 1 and 5 µm. Particle-size of powder B is less than 44 µm and can contain metal traces.

II.2) Elaboration of the samples

This part of the report is related to experimental devices and procedures put in place to make the different samples, from powder treatments to densified materials. Figure 7 is showing a scheme of how the different steps are linked to each other, with the controlled parameters.

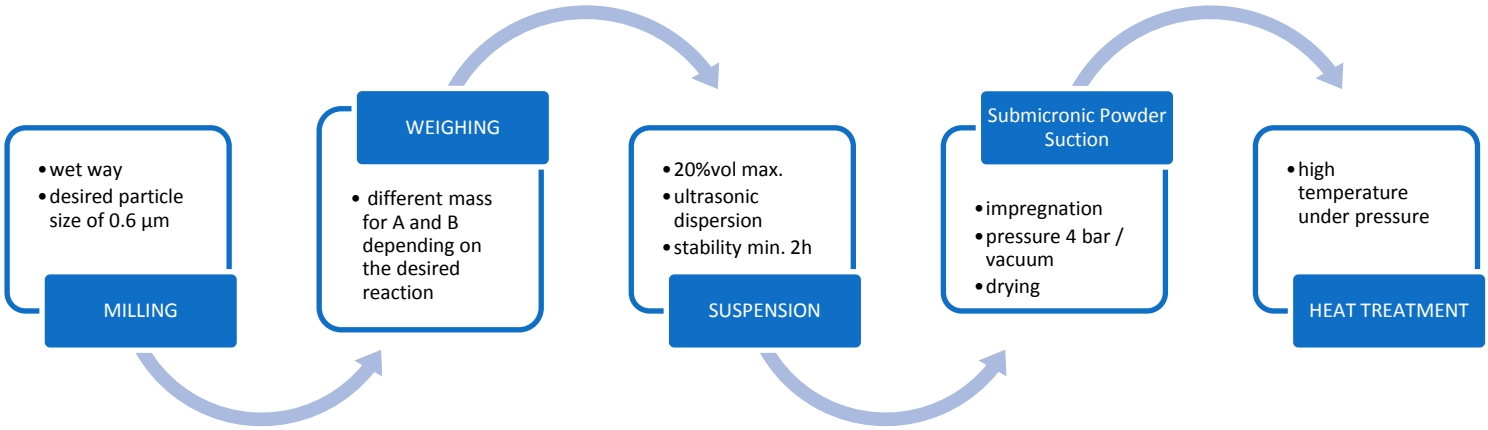

Figure 7 : The different elaboration steps.

II.2.1) Milling of powders for particle size control

As received powders have particle sizes greater than pores' sizes of the fibrous preform in which they have to be introduced. Pore-size distribution is presented in "Characterisation's techniques" part. Hence it is necessary to reduce the powders particle-size. Wet circulation milling technique has been chosen for the following explained reasons.

The milling machine used is a laboratory agitator bead mill of NETZSCH Company (see figure 8) allowing the milling of a solution volume between 70 and 500 mL. The batch can contain a maximum bead volume of 140 mL. Yttria-stabilized zirconia beads with a 0.3 mm diameter were used.

A solution (aqueous or organic, with or without dispersant agent) is conveying the powders. This liquid is stirred in a special bowl and it is being circulated by a peristaltic pump. Then it is conveyed in the air and watertight milling cup which is under pressure and in which the grinding is being possible thanks to the friction of the particles and beads, also bumping into one another. A filter keeps the beads inside the batch. The internal pressure is controlled by a manometer indicating if there is a blockage in the pipes or the batch, or not. A visual inspection is also done at the exit pipe which is opened in the agitator recipient.

Figure 8 : Wet ball milling and circulation device from NETZSCH; source: http://www.netzsch-grinding.com

A cooling system avoids the potential heating up of the grinding devices and also of the circulating fluid. Different parameters are controlled: rotational speed of the milling cup (in rpm, rotation per minute), stirring intensity and circulating speed. Choice of the liquid and addition of dispersant are also influencing powders grinding.

Compared to planetary ball milling or mixer milling, the main interest is to be able to control the particle size distribution all along grinding process, thanks to the open circuit that allows taking samples and analysing them in real time. The next paragraph is presenting the technique used to measure the particle size.

Graphs on figure 9 are presenting the particle size distribution before and after powders milling. Blue curves show the particle size distribution of the commercial powders. It can be observed that size range is from 0.2 to 12 µm for powder A and 0.2 to 10.5 µm for powder B, which shows again the necessity of the milling step before preform impregnation. Several populations are found, for powder A there are 3 of which one is already submicron, and there are 2 populations for powder B with a submicron part.

Final particle size distributions (showed on red curves) are now presenting one and only population, with a mean diameter value (d_{50}) of 0.6 µm. This shows how grinding helped to reduce particle size and to group together the different particle populations.

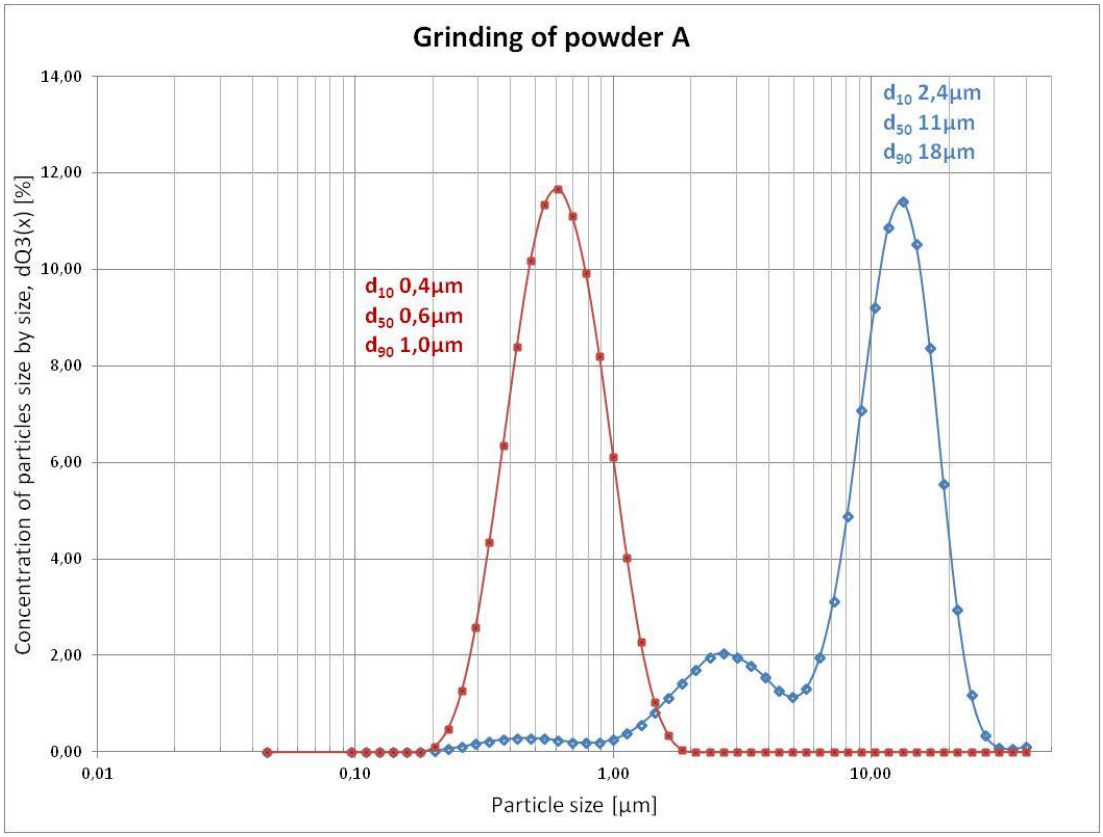

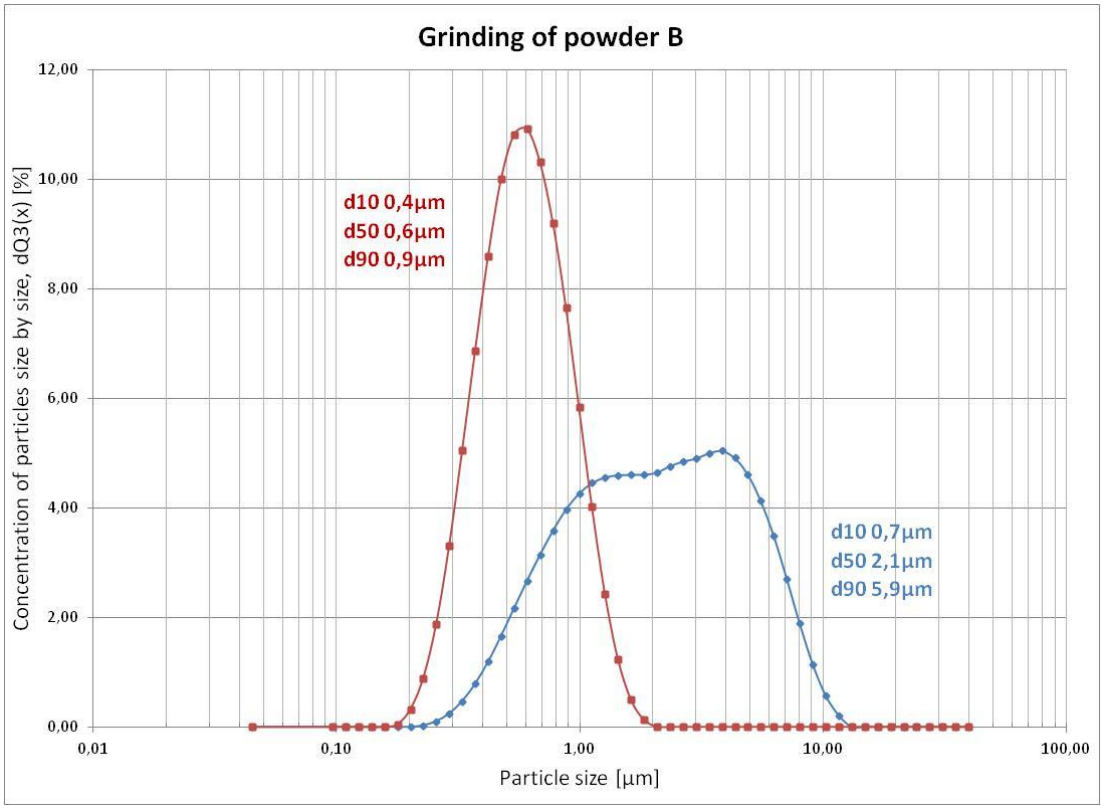

Figure 9 : Particle size distributions for powders A and B, in blue: commercial powders, and in red: powders after milling.

These conclusions can also be observed during SEM observations of the powders before and after milling, which are shown on figure 10. Before milling of powder A, particle size is from 10 to 20 µm with the presence of smaller particles. After milling particles have a homogeneous morphology, and a finer size distribution between 550 and 800 nm.

Same conclusions are made for powder B, but with smaller particle between 2 and 7 µm before milling than for powder A. After grinding, morphologies are similar to the one of powder A with sizes from 280 to 700 nm.

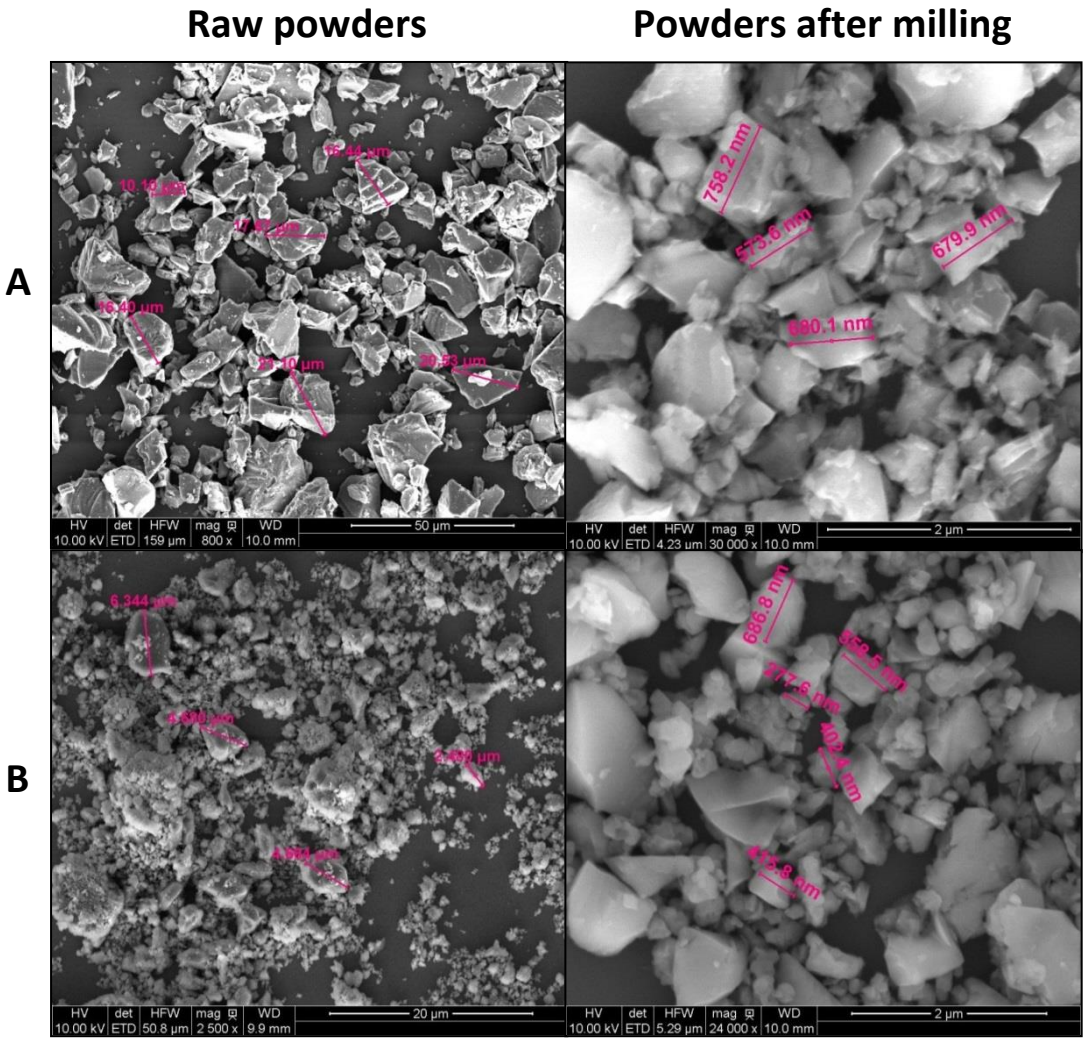

Figure 10 : SEM pictures of raw commercial powders on the left and powders afters milling on the right. Top pictures are corresponding to powder A and bottom pictures to powder B.

II.2.2) Suspension, stability and pH control

The step of particles suspension is really important for the impregnation of the preforms, because it has to be stable during all the duration of the impregnation, to improve and facilitate the particle flow through the porosity to fill the maximum of it. In other cases, like green bodies making, it can prevent from flaws to appear on final densified products [Greenwood, 03]. As the different elements used are confidential, no method of stabilization will be exposed, only the principle and procedures will be described.

- ELECTROSTATIC STABILISATION PRINCIPLE :

During the dispersion of extra fine powder, creation of a liquid-solid interface and presence of free energy in excess are making it thermodynamically unstable. Flocculation occurs in colloidal suspensions when particles are subjected to attractive Van der Waals interactions and Brownian motion because these particles are trying to get a certain kinetic stability. Even if agglomerates and aggregates can be mechanically broken by ultrasonification, it is still necessary to uniformly stabilize the particles in the suspension.

Several mechanisms can avoid flocculation: electrostatic and steric stabilization. It is also possible to combine both in certain cases. Steric stabilization requires the addition of polymers, non-ionic surfactants or proteins that adsorb onto the particle surfaces and are creating a hindered space that blocks the agglomeration of particles. Electrostatic stabilization, also called stabilization by charges, needs the use of charged species, like ions, sufficiently concentrated to stabilize the interactions between particles. This is the technique that has been chosen for this study, because it can be reversible and no elimination treatment for dispersants is needed.

In a polar medium like water, ion pairs dissociate and counter ions together with charged surfaces are forming an electrical double layer. This repulsion caused by entropic phenomenon, has a more or less broad scope in function of the ionic species concentration and can be given by the Debye length κ^{-1} which is given by the following formula:

$$\kappa = \left(\sum_i \frac{\rho_{\infty i} e^2 Z_i^2}{\varepsilon \varepsilon_0 k_B T} \right)^{\frac{1}{2}}$$

where the sum is done on all the ionic species i that are in the system ; $\rho_{\infty i}$ is the i ion concentrations at an infinite distance from the surface ; Z_i i ionic species valence ; kB is Boltzmann constant ; T the temperature ; ε dielectric constant of the particles and ε_0 vacuum permittivity ($8{,}854.10^{-12}$ F.m^{-1}).

Electrostatic repulsion potential between two spherical charged colloidal particles, of radius a and separated from distance r, is obtained by the Poisson-Boltzmann equation:

$$U_{électrostatique}(r) = \left(\frac{64\pi k_B\, T\, a\, \rho_\infty\, \xi^2}{\kappa^2}\right) e^{-\kappa(r-2a)}$$

with $\xi = \tanh\left(\frac{ze\psi_0}{4kT}\right)$; where ρ_∞ is the sum of all the ions' concentrations far from the surfaces and ψ_0 is the particles' surface potential. In this equation it is assumed that the surface potential is independent of the distance r.

Combination of attractive Van der Waals interaction and electrostatic repulsive interaction is known as the DLVO interaction potential (from Derjaguin, Landau, Verwey and Overbeek theory). On figure 11, this model is illustrated taken into account the steric interaction that can occur at short scope when clouds of electrons of surface atoms are coming into contact [Desgritas, 10].

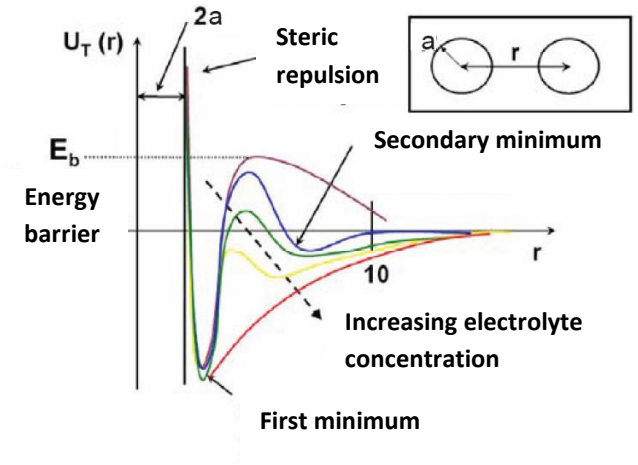

Figure 11 : DLVO interaction potential for different ionic concentrations. Adapted scheme from *F. Thivilliers, Gels d'émulsions à base d'huiles cristallisables : mécanismes de formation et propriétés rhéologiques. Thèse de l'Université Bordeaux 1, 2007*

Control of this mechanism comes through knowing the Zeta potential, which represents a relative value of the particles' charge. Depending on the suspension pH, Zeta potential is varying. Greater the value is, greater is the repulsion. Measurement of this potential is explained later in this report. The following paragraph is detailing the procedure that has been followed to stabilize the suspensions needed for the impregnation step.

- SUSPENSION PROCEDURE :

Powders A and B are introduced in stoichiometric quantity or depending on the mass calculation depending on the treatments and reactions that will occur. The total mass is given by the volume concentration of the suspension that has been fixed empirically. This concentration is giving a low viscosity that provides a good suspension flow through the porosity to get the optimum weight gain. The maximum has been fixed at 18% in volume. Powders are weighed separately and then add progressively in an aqueous solution with a basic pH and mix by magnetic stirring.

PH is measured and stabilised with the addition of TMAH (Tetramethylammonium hydroxide, strong base) and then the suspension is homogenized by ultrasonication to break the agglomerates. These steps are repeated until desired pH is reached to well stabilize the suspension. The suspension has been studied, and pH has been fixed at maximum 9.5 to stabilize it during impregnation which lasts 2 hours.

II.2.3) Submicron powders suction impregnation

Submicron powders suction allow filling of fibrous preforms by combining pressure and vacuum as it is shown on figure 12. This technique has been chosen preferentially to vacuum filling in suspension, even if it is more time consuming.

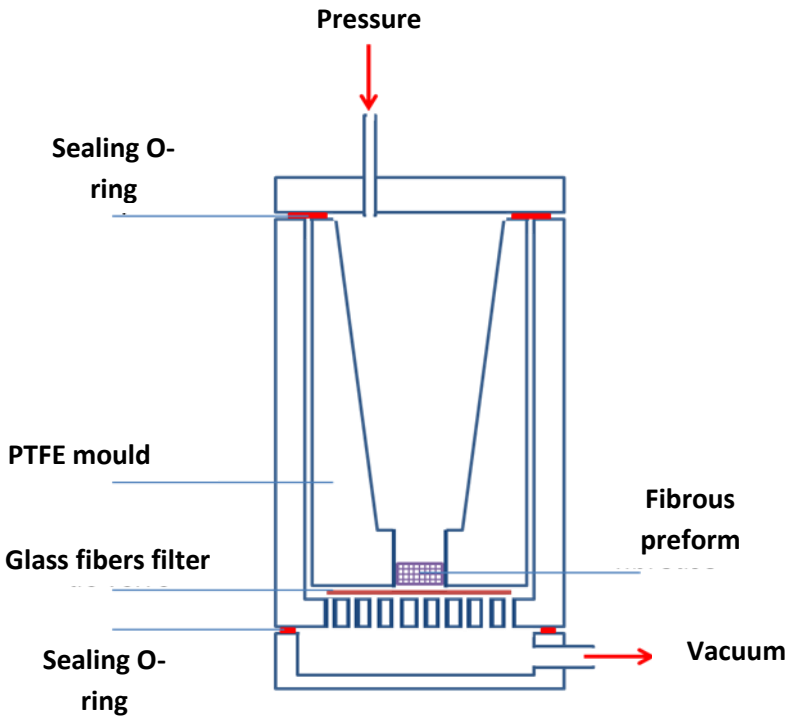

Figure 12 : Scheme of the submicron powder suction device

Impregnation by powder suction allows introducing powders into fibrous preforms' core by applying pressure on the top surface of the sample, and linking the bottom surface to a vacuum chamber. This pressure difference forces the suspension to penetrate the porosity and go through the whole sample. A glass fibre filter, with a special sieve size, is retaining the powders in the preform while the liquid is going in the vacuum chamber. So that particles are blocked in the pores until they are completely filled.

In this work, preforms are already wetted with basic pH water used to prepare the suspensions. This step acts like lubricating of the fibres to improve the access of the porosity by the suspension. The filter is placed at the bottom of the cylinder on the grid, and then the mould and the preform are placed on top of it. It is necessary that all the parts are touching each other to ensure a good air- and water-tightness. The suspension is placed on the preform. When the device is closed and the screws are well tight, if a gas leak is detected, this means that the nitrogen pressure is not applied correctly. If there is no leak for a 2 bar pressure, vacuum is done with a value of -1000 mbar and pressure is set at 4 bar. The impregnation occurs during 2 hours. When the sample is taken out of the mould, it is necessary to remove the surplus of powder on the preform surfaces, because the interest is to fill the maximum intra- and inter-bundlesporosity, not to deposit a few millimetres thick layer.

II.2.4) Pressurised high temperature heat treatment

The secrecy of the subject does not allow communicating in detail on the parameters used, that's why only the experimental device is presented in this part.

The heat treatment reactor, that is used, is presented on the photographs on figure 13. Heat is generated by the Joule effect by applying a current flowing through a Carbon/Carbon resistor which is stuck on two graphite carriers in contact with copper electrodes. The reactor's walls and the copper electrodes are cooling down by different circulation water cooling system. Control medium allow to measure in real time the temperature of the sample using a type S thermocouple (platinum 10% rhodium/platinum) placed the nearest of the sample. A 2-color pyrometer has also been used and is measuring the temperature between 1000 and 2000°C thanks to a hole made on the resistor. Control of the pressure is ensured by manometer and a pressure sensor. The resistor is confined in ceramic felts allowing an electrical isolation with the reactor's walls and thermal isolation to keep the heat around the sample.

A self-regulation program has been set up thanks to a Eurotherm device connected to the thermocouple which controls the heating rates. Then a data acquisition program made with LabView software and connected to the pyrometer, allows to control if the reaction is taking place or not.

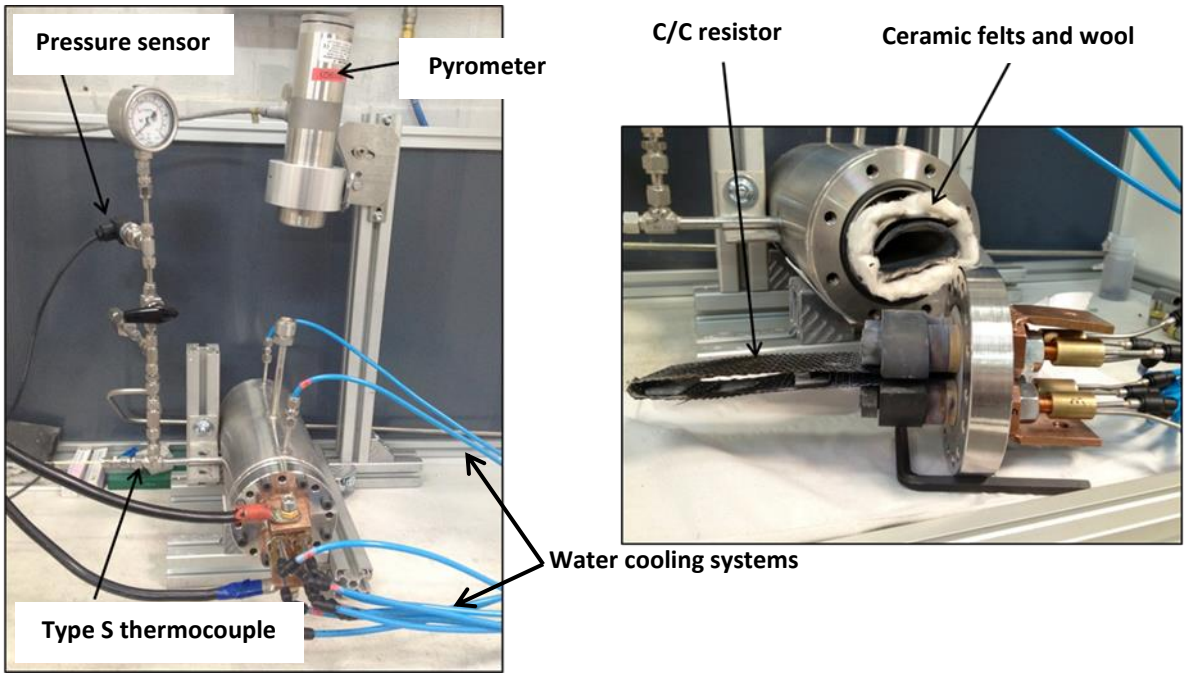

Figure 13 : Experimental device for the pressurised high temperature heat treatment of the dry powder filled preforms.

II.2.5) Experimental plan

To limit the number of experiments, and of course following characterisations on each sample, it has been chosen to study the behaviour of the materials depending on several heating rates (V1<V2<V3…) and only 3 different pressure values (P1<P2<P3). Each combination of parameters has been studied twice, or triple depending on the results, to check the repeatability and reproducibility of the results.

Placements of the sample inside the reactor and the temperature control media had been determining for the experiments. Indeed, a wrong positioning of the sample led to incomplete reaction (see figure 14), while a wrong positioning of the thermocouple led to false control of the temperature and so of the heating rates.

The next part of the report is detailing each characterisation techniques that have been used, their principles of use and the appearances of their results.

Figure 14 : Picture of visible propagation front on incomplete reaction preforms

II.3) Characterisation techniques

Next paragraphs present the different characterisation tools that have been used to analyse the properties of the samples made during all the internship as explained before. Each sample has been subjected to different analysis and tests as listed in the scheme on figure 15. Mechanical testing (traction and micro indentation) has been done on certain samples with different compositions or different treatments selected thanks to previous analysis. But these tests will not be explained in this part because there were some problems during the tests that led to unusable results with imprecise conclusions on their behaviours.

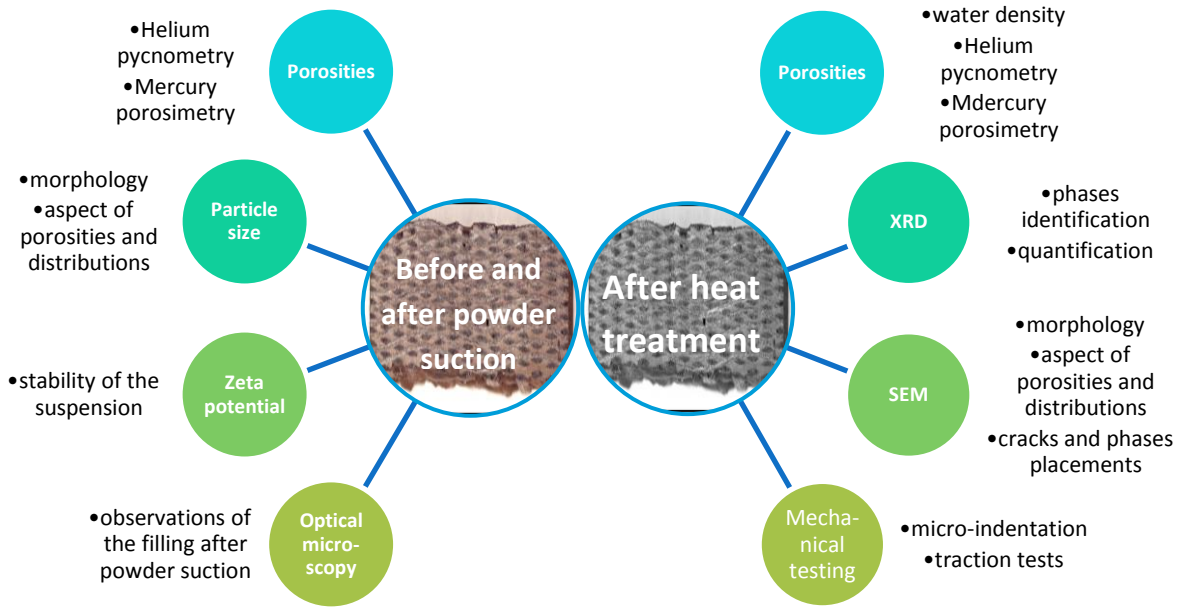

Figure 15 : Scheme of characterisation depending on the treatments that have been done on the samples.

II.3.1) Laser particle sizing

The laboratory is equipped with a laser particle sizer provided by FRITSCH Company, and called ANALYSETTE 22 NanoTec plus (figure 16). The system is composed of a stirring medium for small volumes connected to a pump that makes the solution to flow into the measure unit where can be found the different lasers. These lasers can determine particle sizes with a detection range from 0.01 to 2000 µm and then the distribution is plotted thanks to calculus of size depending on different calculation hypothesis done by MaS Control software.

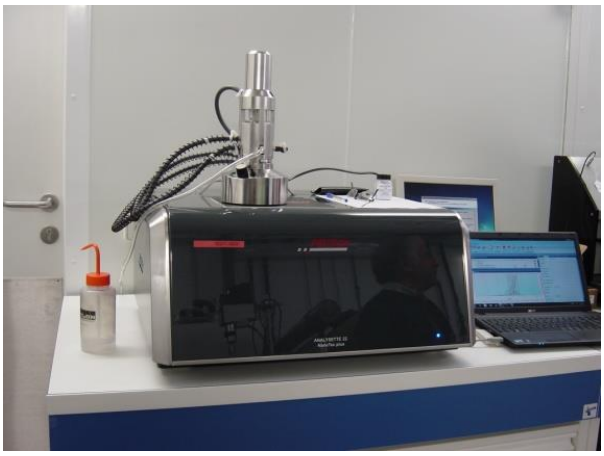

Figure 16 : Fritsch, ANALYSETTE 22 NanoTec plus, laser particle sizer

Three semiconductor laser are used: 2 green lasers (wavelength 532 nm, 7mW) and 1 infrared laser (wavelength 850 nm, 9mW); with a linear polarisation depending on the size range of measurements. In our case only green lasers are used to measure particle sizes between 0.08 and 45 µm. Position of the lasers are represented on figure 17. Measurement principle is based on the relation between the particle size and the diffraction angle of the beam by the particles.

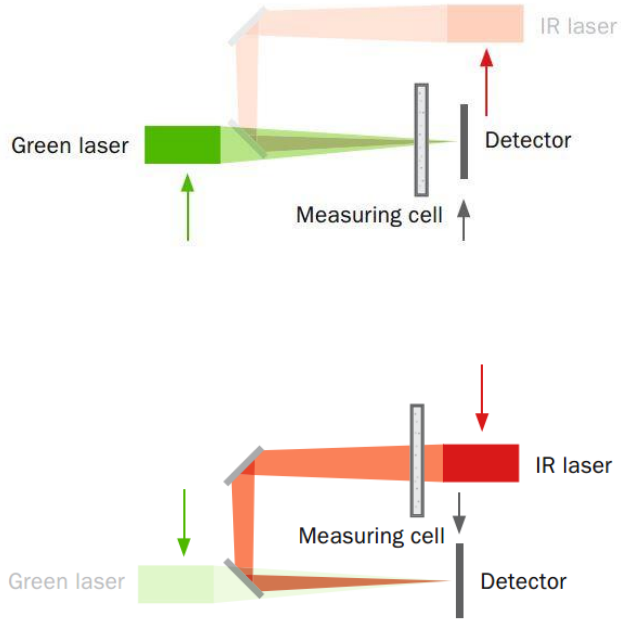

Figure 17 : Positioning of the lasers, green laser for low size ranges and infrared laser for high size ranges

Mie and Fraunhofer theories are used in the software with the possibility to have more or less precise and fine calculations of the distributions. Fraunhofer theory is based on diffraction phenomena and interference effects resulting from light deflection when encountering an obstacle

like a particle in our case. Depending on the light source position, several phenomena occur, like Fraunhofer diffraction when incoming light is parallel. The source can also be considered as located at infinity or shifted by a lens. Mie Theory needs a specific knowledge on optical properties of the materials and the solvent: refraction and absorption index. Particle diameter should be around the wavelength of the light used. The theory is based on Maxwell equations for scattering of electromagnetic waves by spherical particles.

During ball milling, small quantities of suspension are taken. These samples are diluted with the same liquid that the one used for the milling: water or ethanol in our case. Before each measurement and for a better dispersion of the particles when they are going through the analysis cell, ultrasonication is used to break the agglomerates.

The effects of milling are clearly observed on the size distributions of the powders because the mean diameter is decreasing. The concentration of some populations is decreasing because the volume fraction is decreasing. So those low particle size populations are increasing. In many cases, calculations showed unusable results due to calculations errors and also because of the presence of a high particle size population. The mean diameter of this population is around 10 µm and corresponds to agglomerates of particles. Sonication of suspension is needed again to break these agglomerates and to have a distribution closer to reality. These two phenomena are represented on the graph on figure 18 in the boxed areas.

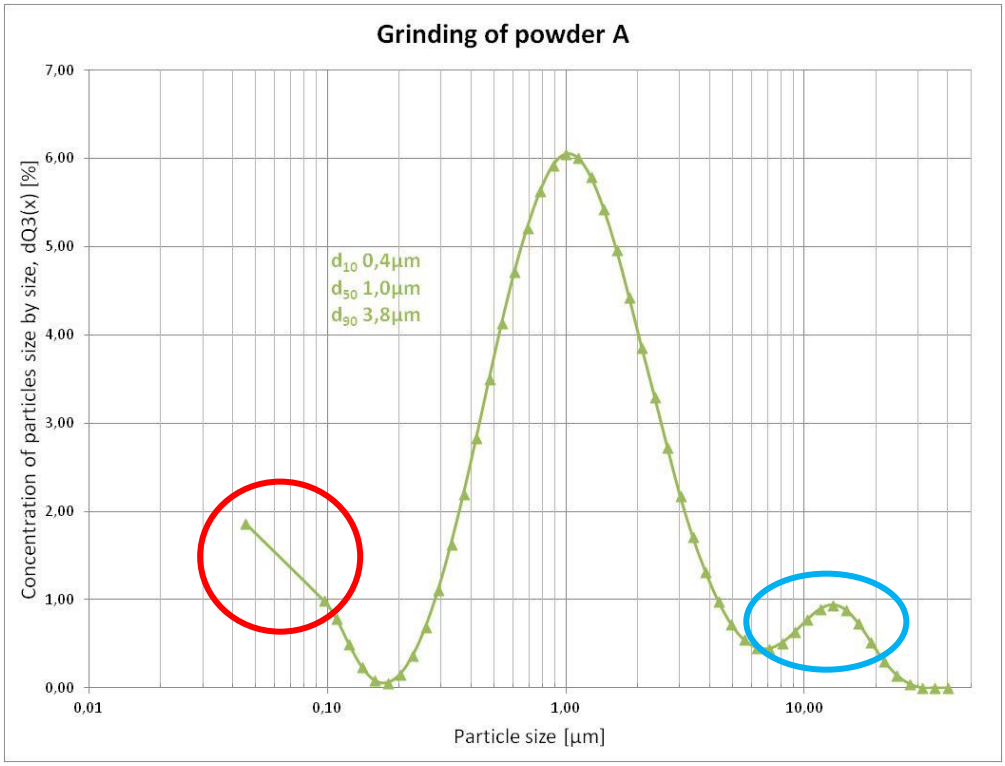

Figure 18 : Particle size distribution of powder A during milling; red framed peak shows calculation errors and blue framed peak shows re-agglomeration population.

II.3.2) Zeta potential measurement

The machine used for measurements is a ZetaProbe Analyzer from Colloidal Dynamics. Samples can be studied up to a concentration of 60% in volume. It also allows zeta potential studies in function of solution pH and also titration studies with the integrated pH-meter. Then the determination of the iso electric point (IEP, pH for which zeta potential equals zero) is possible, as well as a study with flocculating or dispersing agents. Different values are measured: zeta potential, conductivity, pH, temperature, dynamic mobility and iso electric point.

Most of solid's surfaces are electrically charged. At the crystal surface, not all the bonds are saturated. Hence chemisorption phenomena can occur, which is the superficial catch of foreign species (molecules or atoms) by ionic forces. The superficial charge of dispersed particles in water, or in a solution of electrolytes, can become much greater than in air.

These surface charges can result from:

- Partial dissolution of a solid ;
- Ionisation of superficial groups (especially OH^-) ;
- Ion substitution from the crystal lattice of the solid.

These charges are counterbalanced by opposite sign charges coming from other ions in the solution, which is the electroneutrality principle. The electrical double layer is created. The first layer, also called Stern layer, can be formed by positive ions adsorption which are attracted by the negative charges on the particles' surface (like OH^-).

The second layer, also called diffuse layer, is formed with the rest of the ionic charges, moving and dispersed in the solution. Its scope is greater when the surface potential is greater too. In this case, positive ions concentration is more important close to the surface and progressively decreases while getting away from the particle. The boundary between the first and the second layer is called Stern plane.

The Zeta potential is corresponding to the potential difference between particle's surface and Stern plane. It is the only value that can be experimentally measured. Beyond, the electric potential decreases, until it is cancelled at an infinite distance from the particle. Scheme on figure 19 is a representation of these ideas.

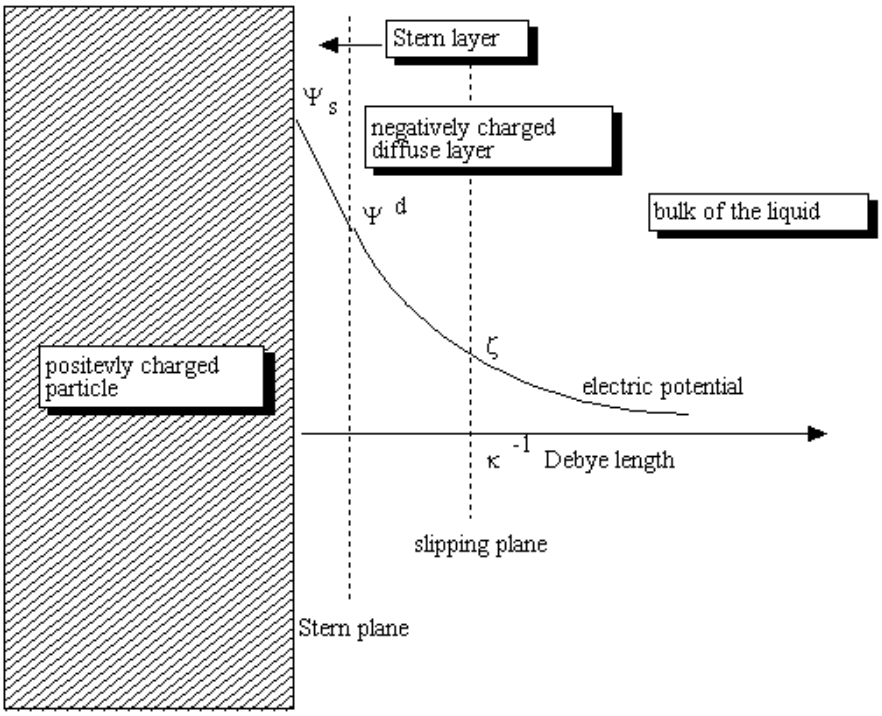

Figure 19 : Scheme of the electrical double layer for a positively charged particle; source: *Wikipedia.com*

The interaction between two particles depends on the potential energy between them and varies in function of the distance between them. The Derjaguin, Landau, Verwey and Overbeek's theory (DLVO) is saying that in a polar liquid, when pH is greater or lower than the iso electric point, the particles are less agglomerated. That means that zeta potential is greater for pH far from the iso electric point pH [Azar, 09].

Greenwood [Greenwood, 00] added that greater is the difference between solution pH and iso electric point pH value, greater is the zeta potential and so more stable is the system. A repulsive barrier corresponding to a zeta potential with an absolute value of 25 mV is necessary to avoid coagulation at 20°C, because the kinetic energy of colloids due to Brownian motions is around 3/2 kT.

Studies of the zeta potential in function of the pH revealed two pH areas which could provide a good stabilization for the suspension. Graphs on figure 20 show studies on powder A and B. Their iso electric points are corresponding to acid pH, so it is better to make the suspension basic to improve stability. A good compromise was found at pH=9, which corresponds to a zeta potential of -60 mV in a 20%vol charged suspension. Moreover, in literature it is possible to find out that a good stabilization is leading to a decreased viscosity of the suspension; in our case it can help improving the impregnation step [Greenwood, 00].

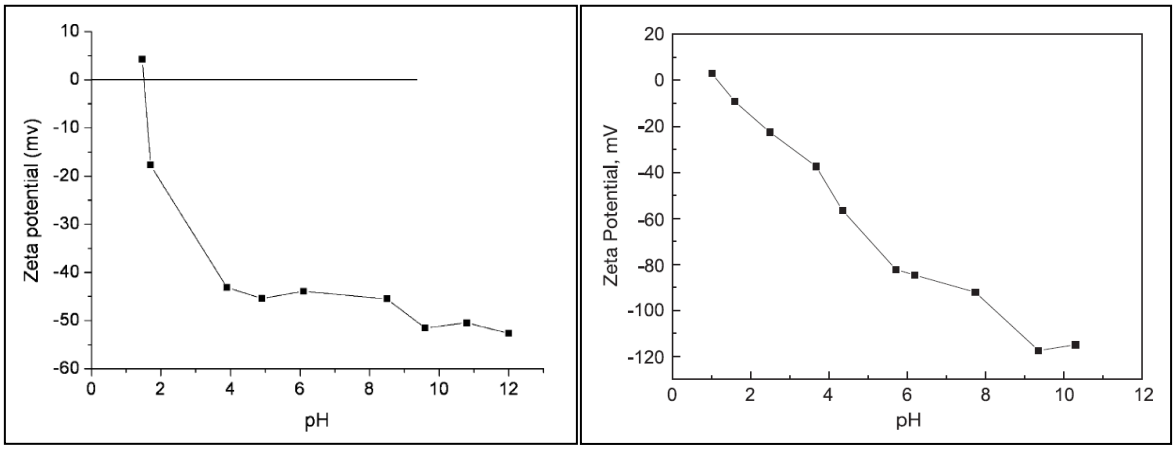

Figure 20 : Studies of zeta potential in function of pH values, powder A on the left and powder B on the right (from two different articles, but references can not be given because of industrial secrecy).

II.3.3) Thermogravimetric Analysis (TGA)

Thermogravimetric analysis, or TGA, aims to study the mass variations of a sample in function of temperature or time under a controlled atmosphere or vacuum. It allows studying the behaviour of materials at different temperature. Different transformations can be detected as for example evaporation, sublimation or oxidation. Each transformation is related to a mass gain or loss. But on the contrary fusion or crystallisation are not influencing the mass, and cannot be detected. For that, further analysis are needed like DTA (Differential thermal analysis) or DSC (Differential scanning calorimetry). TGA is usually destructive for the samples.

A TAG24 TGA machine from SETARAM has been used. Different heating or cooling programs can be used, under inert or reactive atmosphere. It uses a beam balance which is able to record different mass variation ranges of +/- 20 mg for the “low range” and +/- 200 mg for the “high range”. There two symmetrical graphite furnaces equipped with the same devices. On is used as a reference and the other is holding the sample. The scheme presented on figure 21, is showing a device similar to the one that has been used.

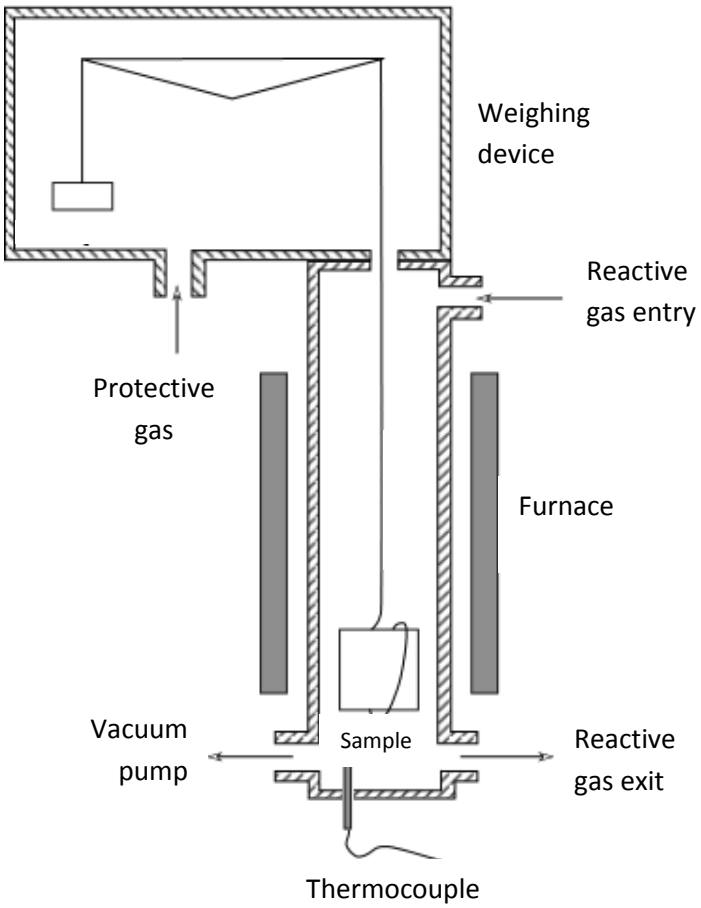

Figure 21 : Functioning scheme of the TGA machine; Source: Wikipedia – Setaram TG-DTA 92 B

II.3.4) Mercury intrusion porosimetry

One of the main steps of the elaboration is the filling of the fibrous preforms with powders. So it has been important to know the pore size distribution of the preforms, to adapt the powder size and then optimize the powder suction process.

Mercury porosimetry is based on the law governing the capillary penetration of a non-wetting liquid inside pores, like mercury. The intrusion pressure is depending on the pores' diameter, so it is possible to determine the pore size distribution of the material. It is calculated thanks to Washburn equation, applying for cylindrical pores:

$$D = -\frac{1}{P} \times 4\gamma \cos\theta$$

with D the pores' diameter, P applied pressure, γ the surface tension and θ the contact angle.

Mercury is not penetrating the pores naturally because of its contact angle which is greater than 90°C. So, smaller are the pores, greater is the intrusion pressure. Mercury volume which is introduced is measured at the same time as the pressure. PV couple is characterizing the porous structure. Calculation hypothesis for the pores' diameter is that pores are considered as cylindrical pores; but most of the porous solids have a more complex geometry with variable sections. The obtained diameters should be taken as pore entry diameter and not the whole pore diameter [Griesser, 12] [Ichard, 02].

The machine used is an AutoPoreIV 9500 produced by Micromeritics Instrument Corporation. Sample is placed in a suitable penetrometer composed of a cup and a capillary stem made of glass which has a metallised surface. This capillary stem is also used to know the volume that has been introduced in the pores in the high-pressure port. That is why it is important to choose the good penetrometer in function of the materials density. If the material is already well densified, a smaller stem has to be used. Pores' volume of the sample should be between 20 and 80% of the capillary volume of the penetrometer. If the chosen capillary tube is too small, the measure will not be correct.

The penetrometer is firstly placed in the low-pressure port, where vacuum is done. Then, mercury is introduced into the cup with a gradual pressure until it reaches 10^5 Pa. At each pressure point there is an associated mercury volume. When the system is back to ambient pressure, the mercury filled penetrometer is placed in the high-pressure port where pressure is applied by oil until 420 MPa. Calculations made by the software give access to density, porosity and pores' size distribution. The machine can give information on pores between 0.003 and 900 µm. The scheme on figure 22 represents the different types of pores in a porous material.

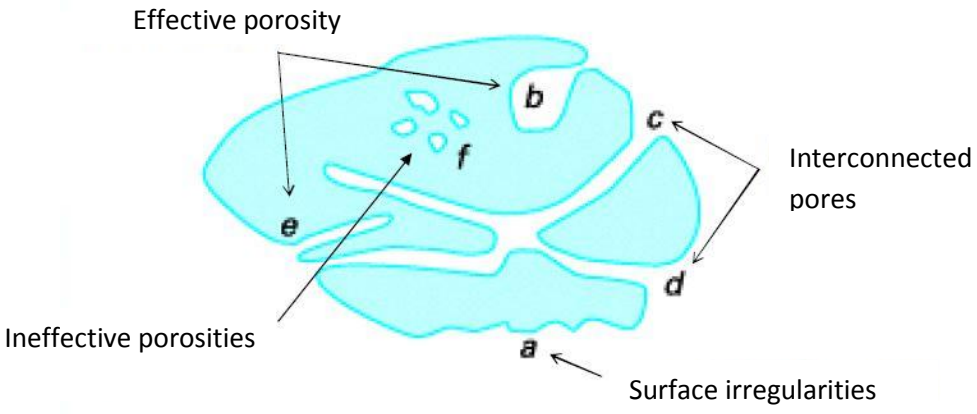

Figure 22 : Scheme of a porous material structure; source: *présentation de la porosimétrie gazeuse et mercure, Gwénaëlle RAIMBEAUX, Laboratoire de Génie Chimique SAP (Service Analyses et Procédés), Université de Toulouse*

Closed porosity, or ineffective porosity, is not accessible by this technique, but high pressures that are used can damaged and lead to the failure of pores' wall which can get to closed porosities. This could be an explanation for strange results. Samples with high roughness are also leading to interpretation mistakes on the porosity, the density or the pores' size.

Another technique of porosity measurement has been used to get an approximate value that was necessary to choose the right penetrometer. It is the helium pycnometry.

II.3.5) Helium pycnometry

Helium pycnometry allows knowing the real volumetric mass density of a solid material by the following formula:

$$D = \frac{m_{sample}}{V_{geometrical} - V_{reaching\ pores}}$$

Helium is penetrating into small pores without fixing the walls because it has no affinity. Because of the closed porosity, there is still a difference between experimental and theoretical values.

AccuPyc 1330 pycnometer from Micromeritics Instrument Corporation has been used. Several analysis cells (10, 35 and 100 cm^3) can be used in function of the sample volume. Scheme on figure 23 presents the working principle. There are two analysis cells linked with a valve. One is holding the sample (V_{cell}) and the other one is the expansion cell (V_{exp}). Helium is firstly injected in the sample cell to get pressure P1. Then the valve is opened and balanced pressure P2 is obtained. Volume is calculated as followed:

$$V_{sample} = V_{cell} - \frac{V_{experimental}}{\frac{P_1}{P_2} - 1}$$

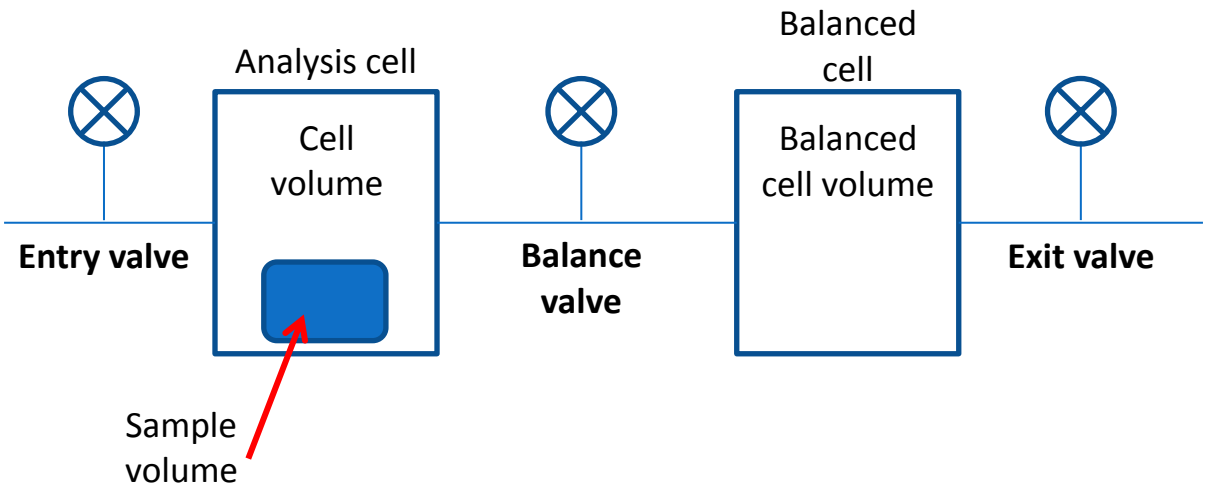

Figure 23 : Working principle scheme of the helium pycnometer

Helium pycnometry can be used to determine densities but also porosity of green bodies or composites, before and after densification thanks to the difference between the real volume (measured volume) and the apparent volume (geometrical volume). For better accuracy, it is important to calibrate the machine before each measurement series thanks to steel beads with a known volume [Griesser, 12] [Ichard, 02].

II.3.6) X-ray Diffraction (XRD)

X-ray diffraction (XRD) is a physical and chemical characterisation technique of the crystalline materials. The diffractometer is a D8 Advance – Bruker AXS. A copper anticathode is generating a beam of X-rays on the sample which is responding depending on the atoms' lattice of its crystalline structure. These answers are recorded by a special linear sensor. Each atom produces a wave that is scattered in all directions, these waves lead to diffraction peaks which depend on the crystal structure. To obtain a diffraction pattern, the X-ray wavelength is the same order of magnitude as the spacing between atoms. There are specific directions, in which the waves are added constructively (see figure 24, for atoms' answers scheme), they can be determined by Bragg's law:

$$2d \sin\theta = n\lambda$$

with d spacing between diffracting planes in nm, θ the incident angle, n refraction index and λ X-ray wavelength nm.

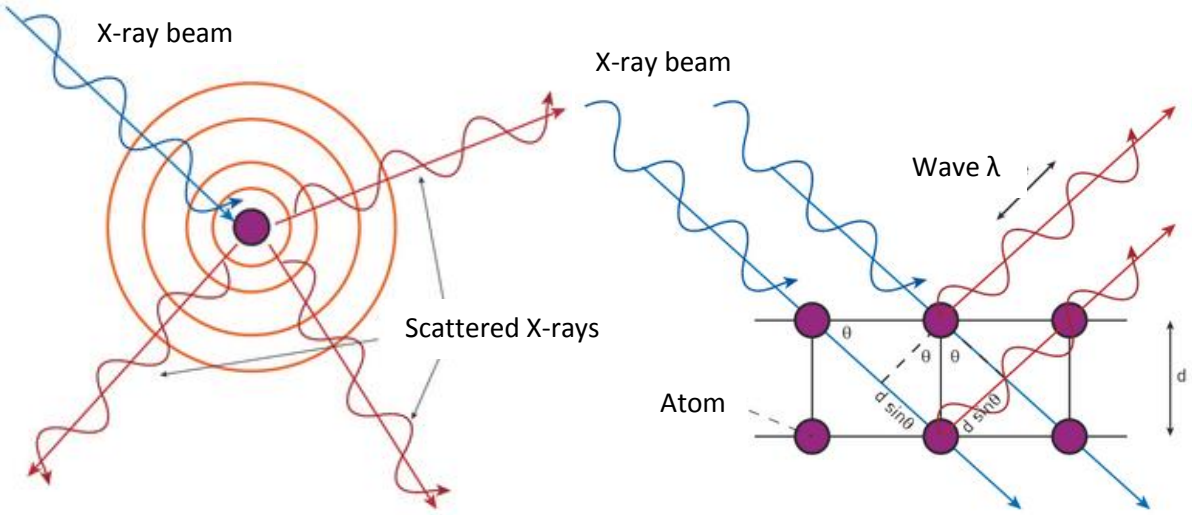

Figure 24 : Atom answering to X-ray beam striking on the left, and waves interactions at crystal scale on the right; source: http://neel.cnrs.fr/spip.php?article1010

Results are obtained as diffractograms on which it is possible to distinguish the different crystal phases in the sample (which can be analysed as powders, green bodies, or densified preforms). Peaks intensity is related to $2\theta$and indicates crystal phase nature. Each peak can be identified alone or combined to other peaks thanks to a database on which a great number of crystal structure are listed. Optimisation of elaboration parameters is based on the development of elements D and E in maximum proportions. That is why it is necessary to quantify these phases on samples made with different parameters, to be able to determine optimum parameters.

To do so, EVA software was used to index the different phases of the materials, and then DIFFRACplus TOPAS software has been used to quantify the phases by Rietveld refinement. It consists of simulating a diffraction pattern from crystallographic models to adapt it to the ones obtained by XRD analysis. This program is taking into account the acquisition parameters as well as structural and crystallographic parameters of the materials that are already known. It is nevertheless an approximate method, but it allowed observing different trends in function of elaboration parameters.

II.3.7) Scanning electron microscopy (SEM)

Scanning electron microscopy (SEM) is a technique which can produce high resolution pictures of samples' surfaces using interactions between electrons and atoms. Scanning electron microscope is composed of an electron gun under vacuum, which produces a fine electron beam pointed at the sample surface which is on a stage plate allowing movements in the 3 space directions. Detectors and sensors are placed around the sample and are recording different signals produced by the sample. In the column, there are condenser lens and deflection coils placed on two perpendicular axes to the beam and that are subjected to synchronized currents which makes the beam scan the surface. The SEM is represented on figure 25.

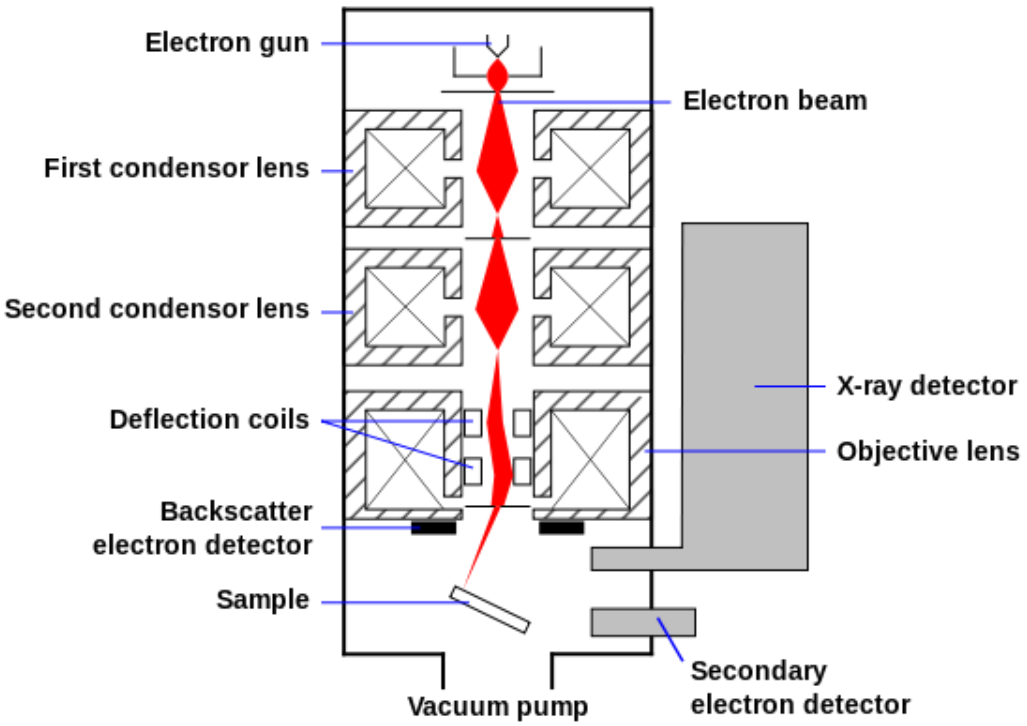

Figure 25 : Schematic of a SEM; Source: Wikipedia

Use of electron, and not photons like for optical microscope, allows reducing wavelengths and having a better resolution. Signals produced by sample surface bring information about the material's nature and surface reliefs. Interaction between electron beam and sample are producing electron emissions with variable energies which are accelerated towards the detectors amplifying the signals. When the beam is striking the sample, electrons are diffusing into a specific volume which is depending on the sample nature. This volume is illustrated on figure 26.

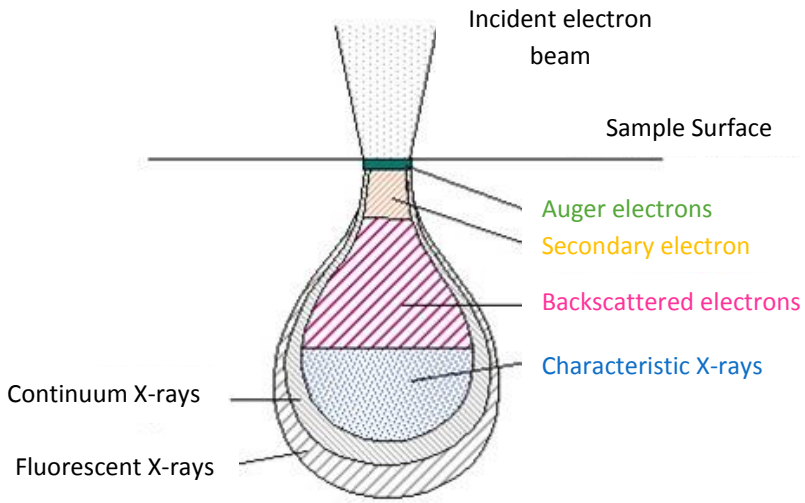

Figure 26 : Interaction volume, « Electron beam interaction diagram ».

In this volume, electrons and electromagnetic rays are used to form pictures or perform physical and chemical analysis. To be detected, rays have to reach the sample surface. Maximum detection depth depends on the ray energy. Following paragraphs are presenting the different particles and rays that are detected, and the information brought by each type.

Schematics on figure 27 present the different types of interaction between electrons and atoms and their paths.

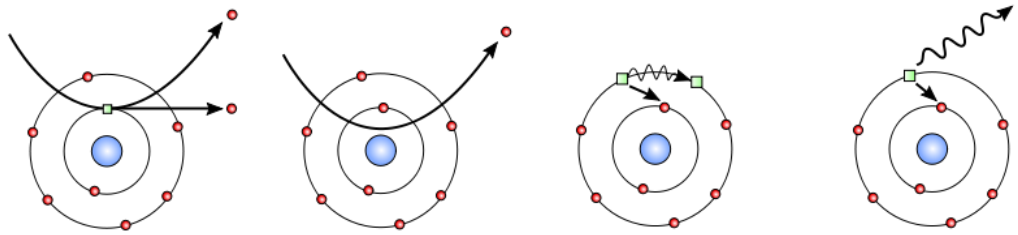

Figure 27 : Interactions electrons-atoms, from the left to the right: secondary electrons, backscattered electrons, Auger electrons and X-ray photon

Secondary electrons have a low energy around 50eV. They are created when primary electron from the electron beam struck an atom. Primary electron is giving a part of its energy to one or several electrons weakly linked to the conduction band. This leads to the ejection of secondary electrons by ionization. These electrons come from the superficial layers, less than 10 nm. They are sensitive to relief variations. Even a small variation is changing the quantity of secondary electrons and gives information on surface topography.

Unlike secondary electrons, **backscattered electrons** are giving information on the chemical species and realize a mapping of the different phases. Their energy is around 30-50 eV. They come from the collision of the beam with atom's nucleus. They are retransmitted in directions closed to their origin direction with low energy loss and coming from greater depth. These electrons are sensitive to the atomic numbers, so that heavy atoms will produce more electrons than light atoms. This can be seen by the contrast between phases on the pictures.

Other atoms with very low energy can be detected, they are called **Auger electrons**. They are emitted by atoms that are already excited due to the electron bombarding and are coming from deep layers. An electron from higher layer comes to fill the gap created by the ejection of the electron, which is releasing energy either by the emission of X-ray photon or given to an electron from a less energetic external orbit. This new electron can also be ejected and detected. Auger electrons are characteristic of the atoms from which they come from. They bring information on the composition and more specifically of the surface and the chemical bonding types. The detector is not found on all SME because of the special conditions needed for the observation.

As explained before, relaxing of electrons can produce **X-ray photons**. They can also be produced when a primary electron with a high energy is ionizing an atom from an internal electronic layer. Analysis of X-rays allows obtaining information on the emitting atom's nature.

Observations were done on a MEBe FEI – Quanta 400 FEG. Extensive analyses were done with different observation modes. Pictures were taken with secondary electrons, backscattered electrons and composition analysis were done with the X-rays detector.

Each sample has been mounted in an Epoxy resin provided by Struers and called Specifix. Polishing has been done with water for plane and fine grinding steps and diamond suspensions for micron polishing cloths, to have perfectly plane and clean surfaces for a better observation of the fibres and the matrix phases. Samples have been gold coated to provide a better source of electrons and to make the surface be conductive. This leads to better observations because it is possible to see more details at higher scale.

III- RESULTS AND DISCUSSION

III.1) Influence of manufacturing steps

III.1.1) Filling of the fibrous preforms by submicron powder suction

As explained previously in this report, experience shows that the volume percent of powders in the solution was influencing the mass gain after impregnation. Depending on the preform type, a suspension with a too high volume percent led to a low mass gain. Experience revealed that for type 1 preform a 18 vol% suspension was providing an efficient filling, and for type 2 preform, which is less porous, only 15 vol% was enough.

- Optical microscope observations:

Photographs on figure 28 are showing a comparison between a preform as it has been received, a preform which has been subjected to a non-optimised impregnation leading to macroporosity in the sample, and finally a preform after impregnation which is reaching 50 to 55% of filled porosity. Too high volume percent suspensions lead to superficial filling because powders cannot reach the heart of the preform. Pores are blocked; suspension flow is limited to pores closed to the surface.

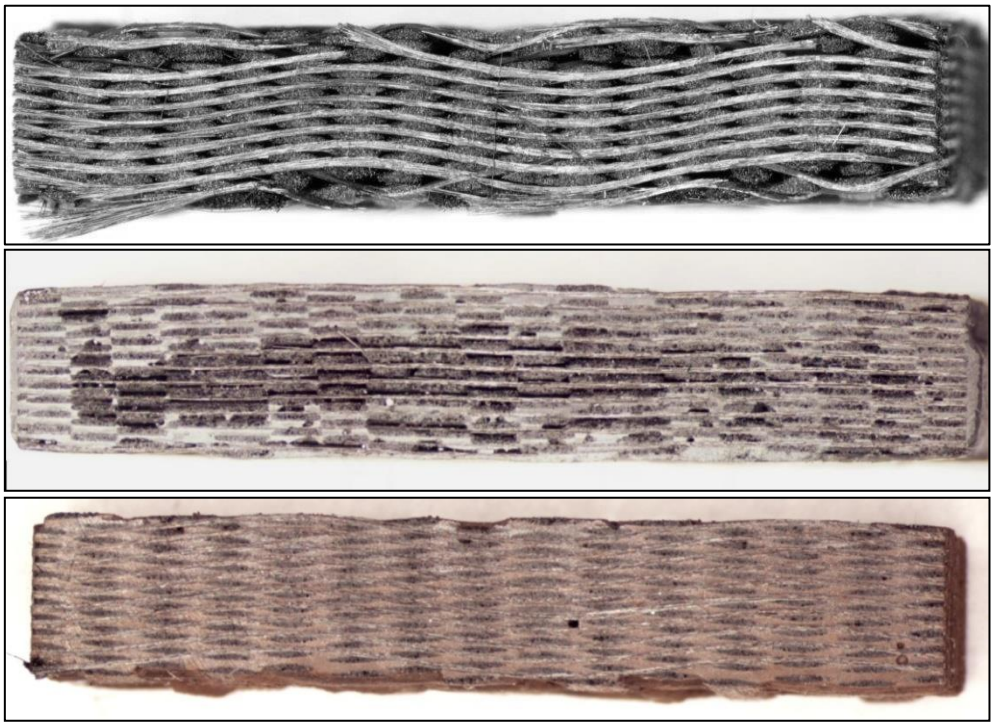

Figure 28 : From top to bottom: non-impregnated preform, preform resulting from a non-optimised impregnation and a preform with 55% of its initial porosity that has been filled by powders.

- Mercury intrusion porosimetry:

Graph on figure 29 shows the pore size distribution of a preform before impregnation. Two populations can be distinguished, one is between 60 and 200 µm and corresponds to the inter-bundlesporosity, and a second one is from 0.8 to 10 µm corresponding to intra-wires porosity.

This analysis shows the necessity of the powder's grinding and explains the choice of the particles' sizes that has been fixed between 0.6 and 0.8 µm, because the smallest pores have an entry size of 0.8 µm as minimum.

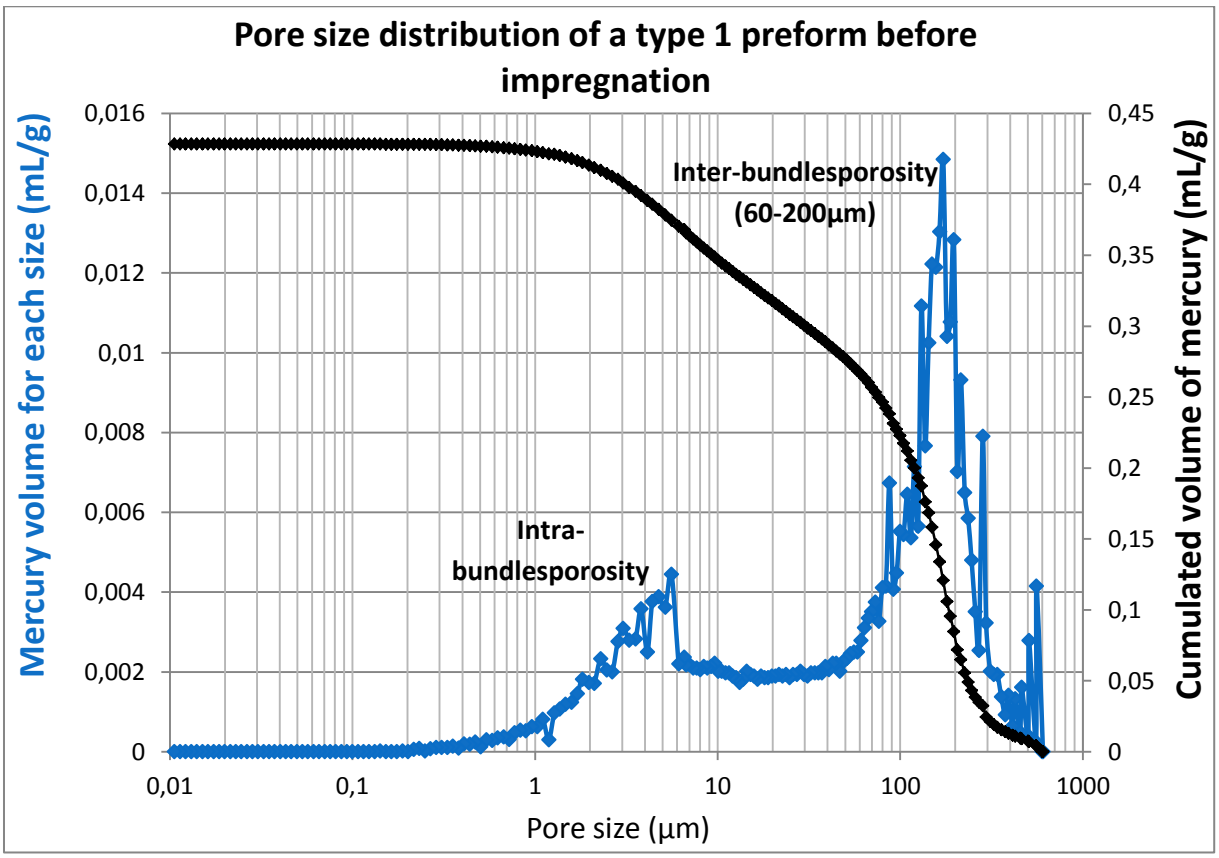

Figure 29 : Pores' size distribution by mercury intrusion porosimetry of a type 1 preform before impregnation.

Graph on figure 30 is now showing the distribution of the pores' sizes after submicron powder suction impregnation. Only one population is found with a mean value of 50 nm, and insignificant variations can be observed between 1 and 10 µm.

Pores' families from inter- and intra-bundlesporosity cannot be observed anymore. This indicates that the filling has been done homogeneously in the whole preform pores. Pores after impregnation have a diameter of around 50 nm for type 1 preform. It is also the case for type 2 preform.

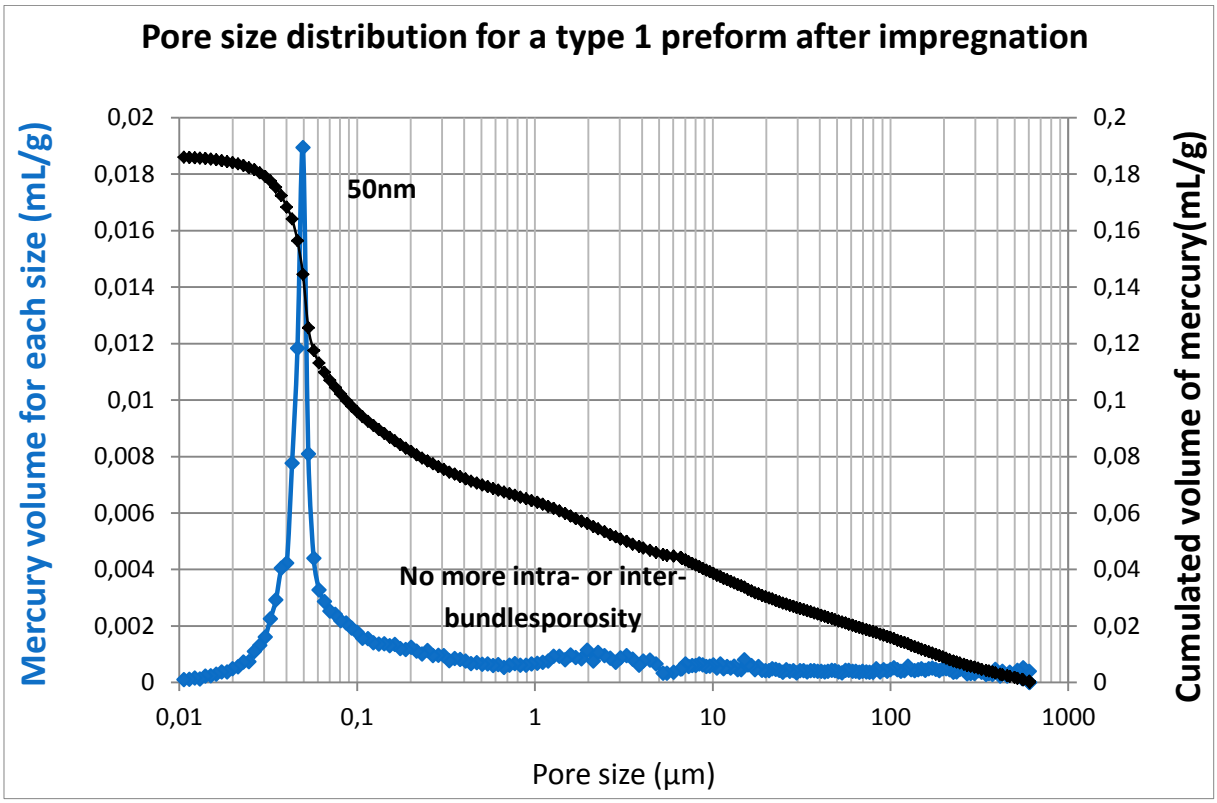

Figure 30 : Pores' size distribution by mercury intrusion porosimetry of a type 1 preform after impregnation.

III.1.2) Pressurised heat treatment

During heat treatment under pressure, impregnated preforms are subjected to high temperatures. Despite, fibres are not damaged. SEM pictures showed any damaging of consolidations, interphases or fibres' cores. One of the pictures that have been taken is shown on figure 31. On can also notice that there is a good cohesion between the matrix and the fibres' consolidations, which is an important aspect for the mechanical behaviour of the composite.

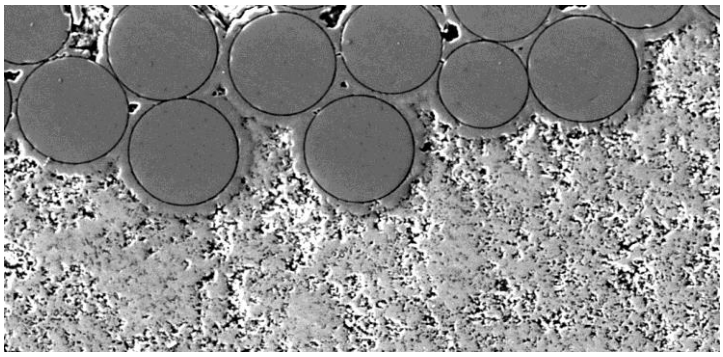

Figure 31 : SEM picture of consolidations, interphases and fibres after pressurised heat treatment.

Moreover, picture on figure 32 is presenting the aspect of the matrix after heat treatment. Powder filling is optimum and homogeneous because the matrix is found everywhere in the pores. Nevertheless, it is noticeable that cracks are induced in the matrix by the heat treatment.

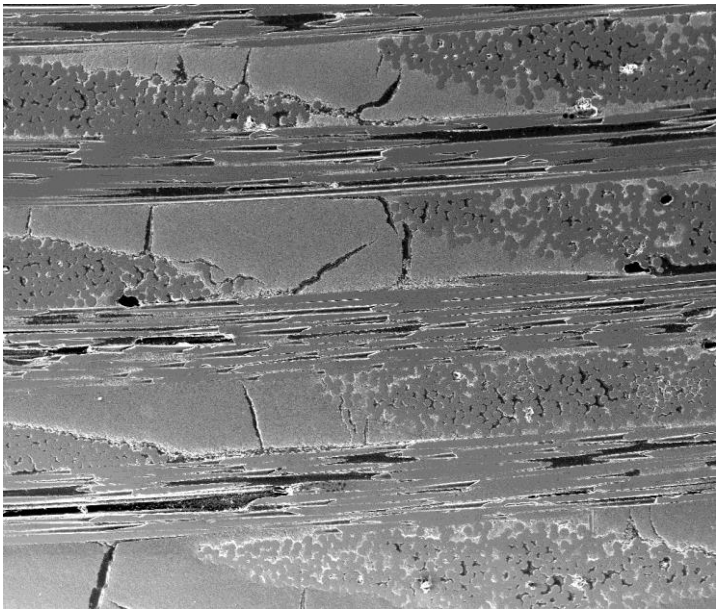

Figure 32 : SEM picture of the matrix after pressurised heat treatment at higher scale.

III.2) Influence of the pressure

The role of the pressure during the heat treatment could have been studied by comparing different thermograms obtained with the collecting of the temperature of the 2-color pyrometer in function of the time.

Several parameters are varying in function of the pressure value, knowing that P1<P2<P3. When the powders are reacting inside the preforms, an exothermal peak is seen on the curves like it is shown on figure 33. When pressure is increasing, the maximum temperature reached by the exothermal peak is also increasing. It can be explained by the thermodynamic activity of the gas that is also increasing. Moreover, the temperature at which the reaction starts is decreasing while pressure is increasing, and it is noticeable that the duration of the exothermal peak is also decreasing.

Three phenomena are highlighted with the thermograms comparison:

- Higher the pressure is, lower the initiation temperature is.
- The peak amplitude is proportional to the gas pressure.
- Higher the pressure is, faster and more intense the reaction is.

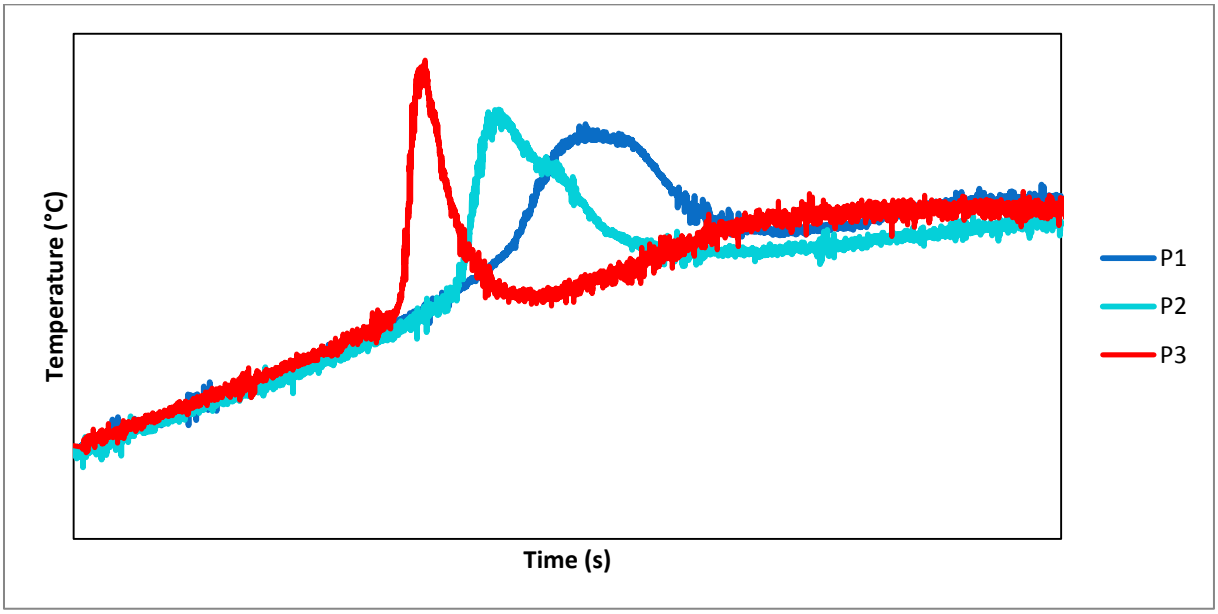

Figure 33 : Comparison of thermograms obtained for a constant heating rate with different pressure values, temperature is measured on the sample surface with a 2-color pyrometer during all the pressurized heat treatment.

Mass quantification that has been done on diffraction patterns obtained by DRX on samples after treatments, also showed variations of the composition in function of the pressure. On figure 34, the graph present the results obtained for a constant heating rate and pressures P1<P2<P3.

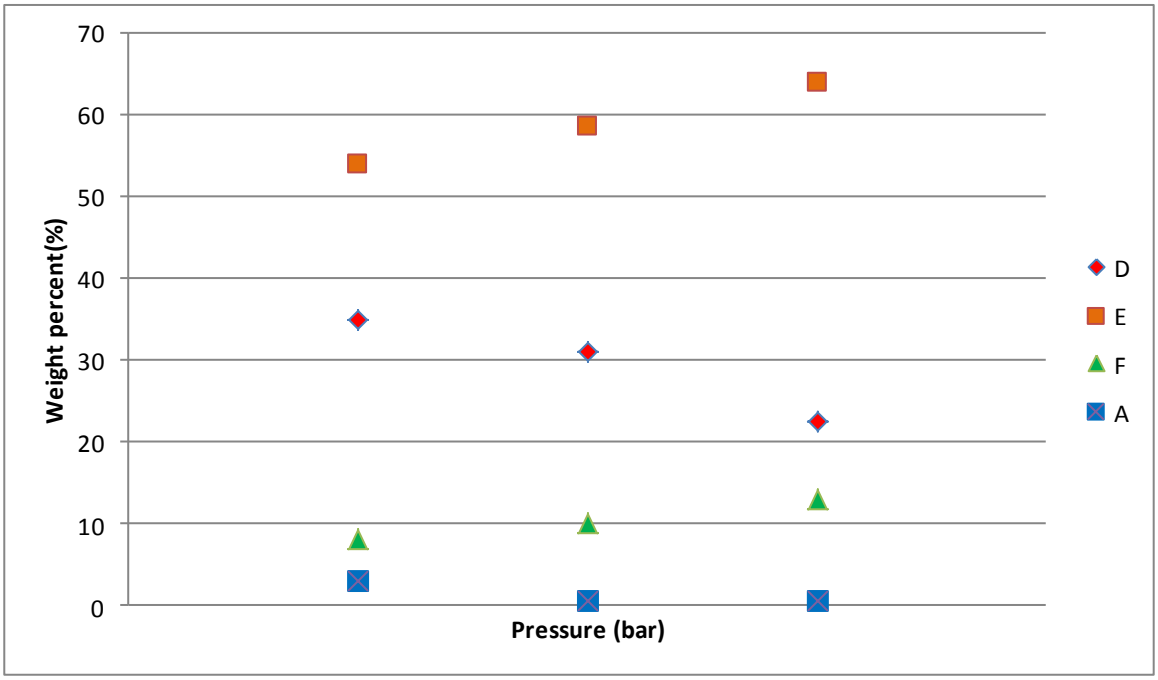

Figure 34 : Evolution of the composition in function of pressure for a constant heating rate.

The reaction that happens, leads to the formation of new components is the following:

$$A + B + C \rightarrow D + E + F$$

Desired components are D and E (same chemical species but two different allotropes). With increasing pressure, E weight percent is increasing while D is decreasing; their sum reaches a maximum for pressure P2. F and A are varying with the same tendency, F increases and A decreases. There are residual traces of initial component A due to its non-reaction or excessive amounts; it is nevertheless low values.

III.3) Influence of the heating rate

Several reactions occur in parallel during the heat treatment, thus it is necessary to determine an efficient heating rate which will lead to the formation of the desired components. SEM observations revealed the presence of particles that did not react for low heating rates. For greater heating rates, these particles are not visible any longer. These no-reaction zones are circled in red on SEM pictures A on figure 35. On the contrary, SEM pictures B on the same figure don't present these zones.

A

B

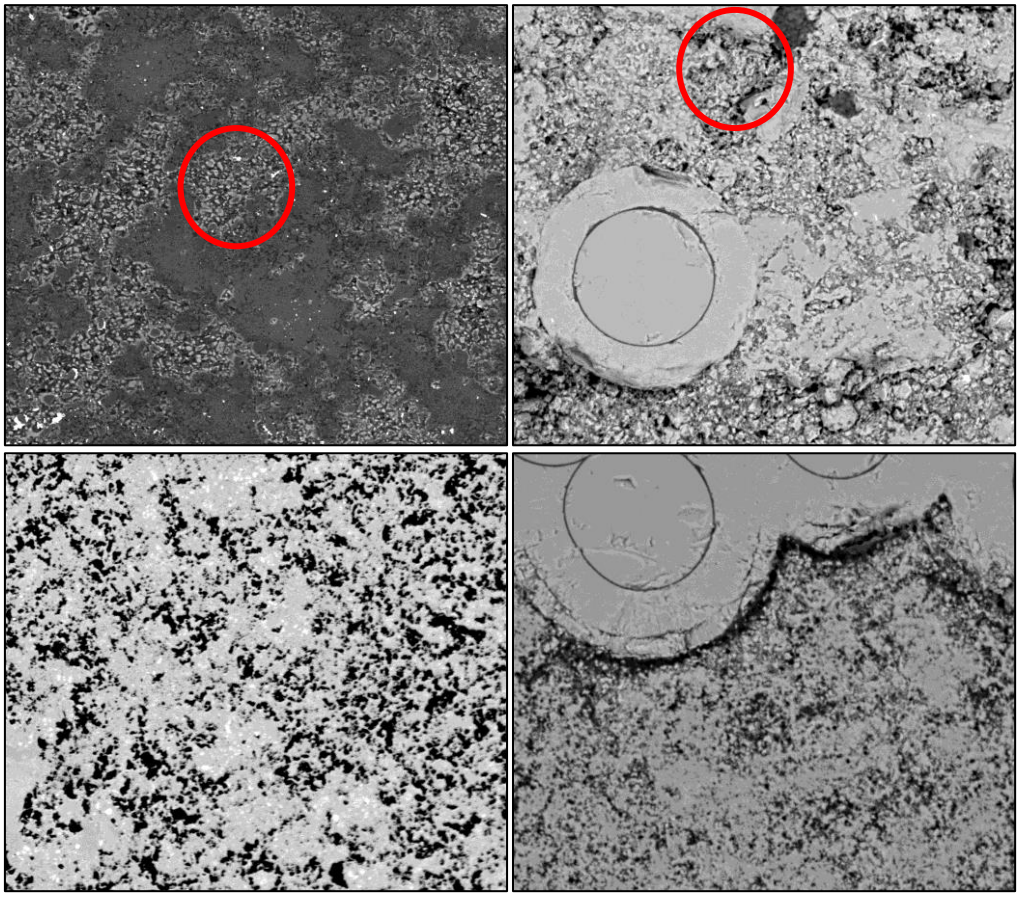

Figure 35 : SEM pictures of the microstructure of composite samples for low (A) and high (B) heating rates; for the same pressure.

Analysis of the composition in function of the heating rates for each pressure showed the same evolution trends (see curves on figure 36). Greater the heating rate is, higher are the D and E phases' weight percent, but F phase is decreasing. For each pressure a balance heating rate, it is increasing while pressure increases:

- For P1 : V1< $V_{balance}$ <V2
- For P2 : V3< $V_{balance}$ <V4
- For P3 : V4< $V_{balance}$ <V5

It is also possible to determine an optimum heating rate for a given pressure leading to the formation of D and E phases. For P1 and P2, V5 seems to be the closest heating rate to the maximum of D and E. But for P3, a higher rate than V6 would be more appropriate.

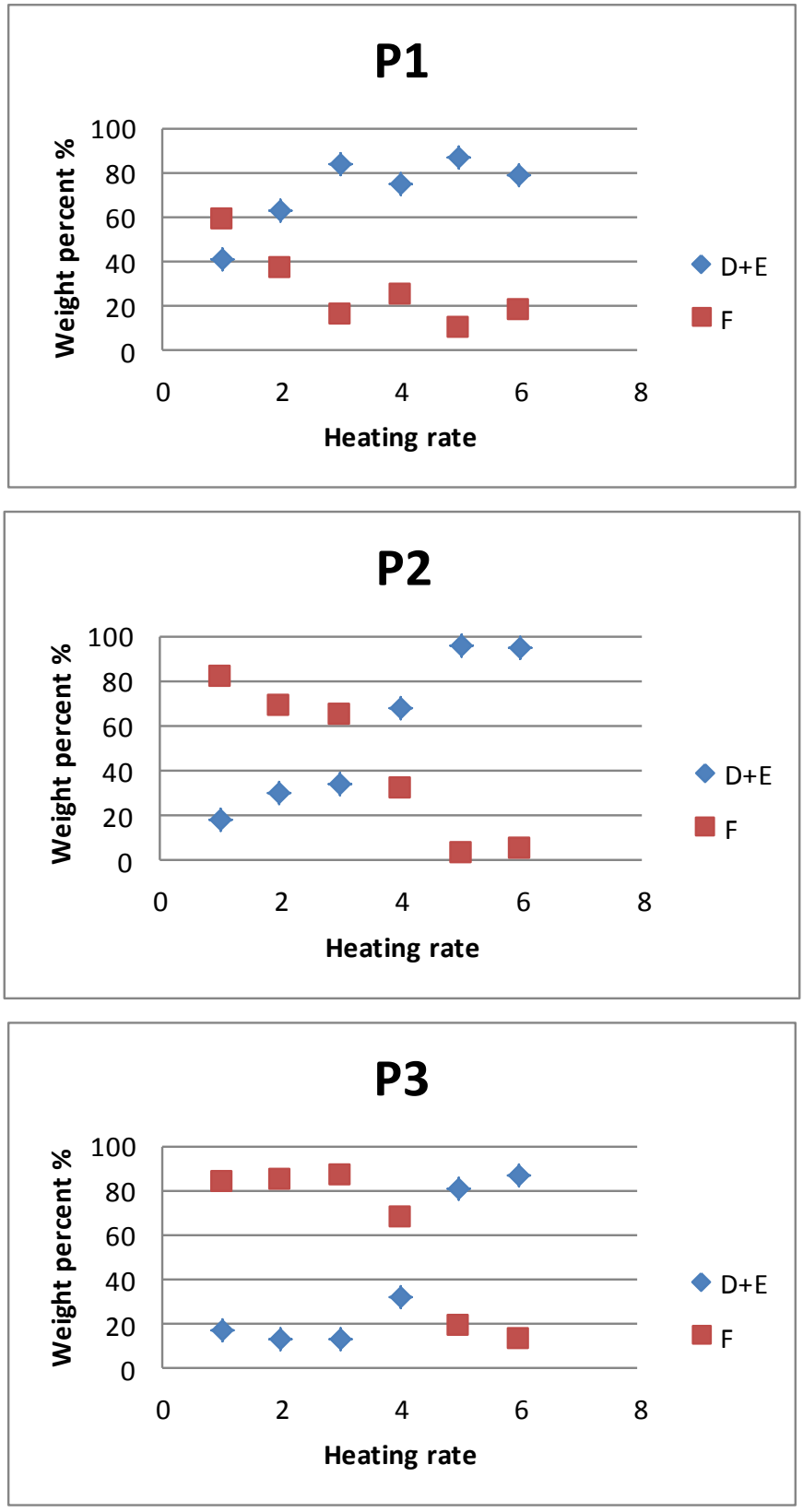

Figure 36 : Evolution of the composition for phases D, E and F in function of the heating rate for pressures P1<P2<P3.

CONCLUSIONS AND SUGGESTIONS FOR FUTURE WORK

During this internship, ceramic matrix composite materials elaboration and characterization, produced by new processes, have been studied. The aim was to improve these processes and optimize the treatments' parameters to obtain the desired materials, to finally be able to get promising characteristics and properties for their use in jet engines of civil air planes. More than 200 samples were made and analysed, allowing a better understanding of certain trends and evolutions of the materials.

Impregnation by submicron powder suction showed its efficiency because only adaptation of the powders mixture's volume percent was needed to be able to fill fibrous preforms with more or less accessible porosity. Nevertheless, wet ball milling was a necessary step to adjust the particles' size. Milling led to a median diameter of 0.6 µm, and then powders were used to make suspensions at 18vol% for type 1 preforms and 15vol% for type 2 preforms.

Pressurised heat treatment has been improved by setting up an automatic control program of the temperature inside the reactor. A collecting data system allows following the evolution of the reaction with the temperature that has been measured on the material surface. Influences of pressure and heating rate on the microstructure, the composition and the porosity were identified. Several combinations of parameters were determined for these CMC materials elaborations depending on the preform type. Heating rate V5 and pressure P2 seemed to give the best results looking at the compositions, because 95wt% were reached for the desired constituents.

The characteristics of the silicon carbide fibres that have been used, are important parameters to take into account for this kind of elaboration. Indeed, temperatures reached, even for a brief moment, are exceeding the thermal stability of Nicalon and Hi-Nicalon, and can damage their mechanical properties. Only pure SiC fibres can tolerate this increase of temperature. However, ceramic fibres are subjected to high temperature only for a short time. This is the main interest of this process, materials synthesis at high temperature, sometimes close to the limit of thermal stability of Hi-Nicalon S fibres, but for a short time that is limiting the damage and degradation of the mechanical performances.

The optimisation and improvement of these processes led to the determination of the key parameters for the formation of 95wt% of the desired ceramic constituent. To have a more complete knowledge on the material's properties, mechanical testing has been done which are micro indentation and traction testing. But because of some problems during the assays, results could not be used entirely or data could not have been collected at all. It is important to continue with these tests and determine exactly the good procedures that have to be followed for the samples preparation to be able to compare results with one other. Knowing their desired use in severe conditions, oxidation and aging studies are an interesting point that requires further research.

REFERENCES

[Azar, 09] M. Azar. Mise en forme et frittage des poudres céramiques nanostructurées: cas d'une alumine de transition. Thèse de doctorat, Institut National des Sciences Appliquées de Lyon, 2009.

[Baïlon, 00] J. P. Baïlon *et al*. Des matériaux, 3ème édition. Presses internationales polytechniques, 2000.

[Bouillon, 91] E. Bouillon *et al*. Composition-microstructure-properties relationships in ceramic monofilaments resulting from the pyrolysis of a polycarbosilane precursor at 800°C to 1400°C. Journal of Materials Science, vol. 25, p. 1517, 1991.

[Bunsell, 00] A. R. Bunsell *et al*. Fine diameter ceramic fibres. Journal of the European Ceramic Society, vol. 20, p.2249, 2000.

[Bunsell, 05] A. R. Bunsell. High-performance fibers. Encyclopedia of materials : Science et Technology (Second Edition), p. 1-10, 2005.

[Bunsell, 06] A. R. Bunsell *et al*. A review of the development of three generations of small diameter silicon carbide fibers. Journal of Material Science, vol. 41, p823, 2006.

[Chollon, 95] G. Chollon, « Fibres céramiques à base de carbure de silicium et à faible taux d'oxygène ». Thèse de doctorat, université Bordeaux 1, 1995.

[Choy, 03] K. L. Choy. Chemical vapor deposition of coating. Progress in Materials Science, vol. 48, p. 57, 2003.

[Christin, 02] F. Christin. Design, fabrication, and application of thermostructural composites (TSC) like C/C, C/SiC, and SiC/SiC composites. Advanced Engineering Materials, vol. 4 (12), p. 903, 2002.

[Christin, 05] F. Christin. A global approach to fiber nD architectures and self-sealing matrices : from research to production. International Journal of Applied Ceramic Technology 2, vol. 2, p.97, 2005.

[Desgritas, 10] M. Desgritas. Emulsions stabilisées par des particules colloïdales stimulables : propriétés fondamentales et matériaux. Thèse de doctorat, Université de Bordeaux 1, 2010.

[Dong, 02] S. M. Dong *et al*. Microstructural evolution and mechanical performances of SiC/SiC composites by polymer impregnation/microwave pyrolysis (PIMP) process. Ceramic International 8, vol. 28, p. 899, 2002.

[Duan, 12] L. Duan *et al*. Effect of pyrolysis temperature on the pore structure evolution of polysiloxance-derived ceramics. Ceramics international 38, p. 2667, 2012.

[Dupeux, 04] M. Dupeux. Science des matériaux. Editions Dunod, Paris, 2004.

[Eberling-Fux, 06] N. Eberling-Fux. Matériaux composites à matrice nanostructure dans les systèmes Si-B-C-Ti et Si-B-C-N. Thèse de doctorat, Université de Bordeaux 1, 2006.

[Gay, 97] D. Gay. Matériaux composites 4ème édition revue et augmentée, Hermès, 1997.

[Greil, 00] P. Greil. Polymer derived engineering ceramics. Advanced engineering materials, vol. 6, p. 2, 2000.

[Greenwood, 00] R. Greenwood. Acoustophoretic studies of aqueous suspensions of alumina and 8mol% yttria stabilized zirconia powders. Journal of the European Ceramic Society, vol. 20, p.77-84, 2000.

[Greenwood, 03] R. Greenwood. Review of the measurement of zeta potentials in concentrated aqueous suspensions using electroacoustics. Advances in Colloid and Interface Science, vol. 106, p.55-81, 2003.

[Griesser, 12] A. Griesser. Réalisation de matériaux composites à conductivité thermique accrue pour l'aéronautique. Thèse de doctorat, Université de Bordeaux 1, 2012.

[Gumula, 04] T. Gumula *et al*. Structural characterization of polysiloxane-derived phases produced during heat treatment. Journal of Molecular Structure 704, p. 259, 2004.

[Ichard, 02] J-C. Ichard. Composites à matrice céramique à conductivité thermique améliorée. Thèse de doctorat, Université de Bordeaux 1, 2002.

[Ichikawa, 00] H. Ichikawa. Recent advances in nicalon ceramic fibres including Hi-Nicalon Type S. Annales de Chimie Science des Matériaux, vol. 25, p.532, 2000.

[Kevorkijian, 99] V. M. Kevorkijian. The reactive infiltration of porous ceramic media by a molten aluminium alloy. Composites and Science and Technology, vol. 59, p. 683, 1999.

[Lamouroux, 99] F. Lamouroux *et al*. Oxidation-resistant carbon-fiber-reinforced ceramic matrix composites. Composites Science Technologie, vol. 59, p. 1073, 1999.

[Lécrivain, 87] L. Lécrivain. Céramiques. Généralités. Techniques de l'Ingénieur. 10/02/1987. A7290.

[Luthra, 93] K.L. Luthra *et al*. Toughened Silcomp composites – Process and preliminary properties, American Ceramic Society Bulletin 72, p. 79, 1993.

[Naslain, 98] R. Naslain. The design of the fibre-matrix interfacial zone in ceramic matrix composite. Composites Part A 29A, p. 1145, 1998.

[Naslain, 99] R. Naslain. Matériaux pour les aéronefs : de plus en plus de composites structuraux et thermostructuraux. Lettres des sciences chimiques du CNRS – L'actualité chimique, 1999.

[Naslain, 01] R. Naslain *et al*. Synthesis of highly tailored ceramic matrix composites by pressure-pulsed CVI. Solid State Ionics 141-142, p. 541, 2001.

[Naslain, 03] R. Naslain, F. Christin. SiC-matrix composite for advanced jet engine. MRS Bulletin, p.654, 2003.

[Naslain, 04] R. Naslain. Design, preparation and properties of non-oxide CMCs for application in engines and nuclear reactors : an overview. Composites Science and Technology, vol. 64, p155, 2004.

[Naslain, 05] R. Naslain. SiC-matrix composite nonbrittle ceramics for thermostructural application. International Journal of Applied Ceramic Technology 2, vol. 2, p.75, 2005.

[Papakonstantinou, 01] C. G. Papakonstantinou *et al*. Comparative study of high temperature composites. Composites part B, vol. 32, p. 637, 2001.

[Penas, 02] O. Penas. Etude des composites SiC/SiBC à matrice multiséquencée en fatigue cyclique à hautes températures sous air. Thèse de doctorat, Université de Bordeaux 1, 2002.

[Qi, 05] G. J. Qi *et al*. Preparation of three-dimensional silica fiber reinforced silicon nitride composites using perhydropolysilazane as precursor. Materials Letters 59, p. 3256, 2005.

[Shimada, 95] S. Shimada *et al*. Formation and microstructure of carbon-containing oxides scales by oxidation of single cristals of zirconium carbide. Journal of the American Ceramic Society 78, vol. 1, p. 41, 1995.

[Taillet, 14] B. Taillet. Procédés alternatifs pour l'élaboration de matériaux composites à matrice céramique. Thèse de doctorat, Université de Bordeaux 1, 2014.

[Takeda, 95] M. Takeda *et al*. High performance silicon carbide fiber Hi-Nicalon for ceramic matrix composite. Ceramic Engineering & Science Proceedings, vol. 16, p. 37, 1995.

[Takeda, 98] M. Takeda *et al*. Microstructure and oxidative degradation behavior of silicon carbide fiber Hi-Nicalon type S. Journal of Nuclear Materials 258, p. 1594, 1998.

[Tampieri, 92] A. Tampieri *et al*. Oxydation resistance of alumina-titanium nitride and alumina-titanium carbide composites. Science and Technology of Advanced Materials, vol. 6, p. 1688, 1992.

[Yajima, 76] S. Yajima *et al*. Synthesis of continous SiC fiber with high tensile strengh. Journal of the American Ceramic Society, vol. 59, p324, 1976.

[Yajima, 78] S. Yajima *et al.* Synthesis of continuous silicon carbide fiber with high tensile strengh and high Young's modulus. Journal of Materials Science, vol. 13, p2569, 1978.

[Wang, 98] C. Wang *et al*. The effect of whiskers orientation in SiC whiskers reinforced Si3N4 ceramic matrix composites. Journal of the European Ceramic Society, vol. 19, p.1903, 1998.

[Ziegler, 99] G. Ziegler *et al*. Fiber reinforced composites with polymer derived matrix, processing, matrix formation and properties. Composites : Part A 30, p. 411, 1999.